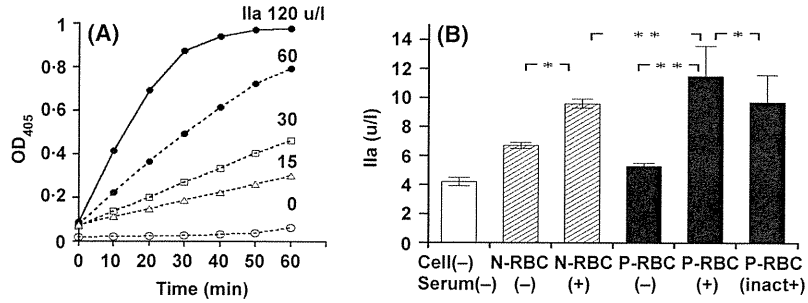

Fig 1. Procoagulant properties of the supernatants of C′-activated RBC in sucrose buffer. Panel A: Enzymatic assay for IIa was employed for the measurement of IIa generation in diluted plasma. Calibration curve generated by serially diluted bovine α IIa shows the linear relationship between time (0–60 min) and absorbance in a range of IIa (0–60 u/l) added to wells containing IIa-specific chromogenic substrate. Panel B: The supernatants of C′-activated PNH-RBC (P-RBC) in sucrose buffer showed enhanced procoagulant properties more than those of normal RBC (N-RBC) similarly treated or PNH-RBC treated with inactivated serum. Only the supernatant of C′-activated PNH-RBC showed apparent haemolysis in this experiment. Bars indicate the mean ± SD of triplicate assays. This figure shows data for Patient 1. $^{*}P < 0{\cdot}05$; $^{**}P < 0{\cdot}01$.

the samples (PS-containing supernatants) were incubated with Annexin V-streptavidin-coated microplates and allowed to bind to the plates; then IIa generated from prothrombin by the action of Xa–Va (prothrombinase) added to the wells was enzymatically measured. PS-exposed MPs accelerate IIa generation. Assays were performed exactly according to the manufacturer's instructions. Results are expressed as PS concentration by calculation from the calibration data of standard PS material included in the assay kit.

PKC activation and inhibition of RBC for IIa-generation assay

PKC activation of RBC was induced by treatment of RBC, normal and PNH, with PMA (0·1 μmol/l, 23°C, 30 min) in HEPES-buffered saline, 145 mmol/l NaCl, pH 7·4, containing 2 mmol/l $CaCl_2$. PKC inhibition of RBC was induced by preincubation of RBC with Calphostin C (1·67 μmol/l, 37°C, 30 min).

FCM

PS-exposed MPs or PS-exposed RBC upon C′-activation were analysed using an Annexin V-FITC Apoptosis Detection kit (Sigma). Aliquots (50 μl) of samples (RBC suspensions after C′ activation in sucrose buffer) were added to test tubes containing 1× binding buffer (10 mmol/l HEPES/NaOH, pH 7·5, containing 140 mmol/l NaCl and 2·5 mmol/l $CaCl_2$), and then 1 μl Annexin V-FITC conjugate was added. After a 10-min incubation at 23°C, samples were analysed by FCM. For some experiments, RBC were pretreated (30 min, 23°C) with PKC inhibitors (10 μmol/l Calphostin C or 100 nmol/l Ro-31-8220), calpain inhibitors or a caspase inhibitor, and then treated by C′ activation. To clarify the effects of Ca^{2+} on MP generation, 2 mmol/l chelating agents, either ethylene glycol-bis(2-aminoethylether)-*N*,*N*,*N*′-*N*′-tetra-acetic acid (EGTA) or 2 mmol/l ethylenediaminetetraacetic acid (EDTA), were added to the C′-activation condition in the sucrose buffer containing 1 mmol/l $MgCl_2$.

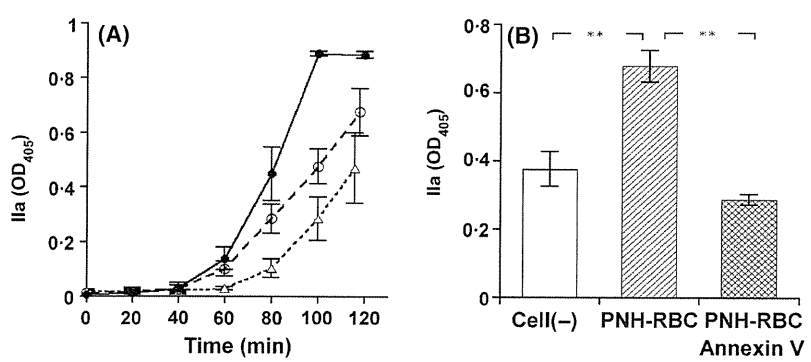

Fig 2. Procoagulant alteration of PNH-RBC by C′ activation. Panel A: IIa generation (OD_{405}) in diluted plasma was measured enzymatically using IIa-specific chromogenic substrate. The presence of PNH-RBC (black circle) that were C′-activated in sucrose buffer, accelerated the coagulation process in diluted plasma in comparison with the presence of normal RBC (open circle), which were treated the same, or under cell-free conditions (open triangle). Panel B: When IIa generation in diluted plasma at 100 min was compared, the enhanced IIa generation in the presence of C′-activated PNH-RBC was diminished by their subsequent treatment with annexin V (10 μg/ml, 23°C, 30 min). Horizontal bars indicate the mean ± SD of triplicate assays. This figure shows data for Patient 2. $^{**}P < 0{\cdot}01$.

Data analysis and statistics

Data were analysed using graphical data analysis software packages, Microsoft Excel (Seattle, WA, USA) and KALEIDA GRAPH (Synergy Software, Reading, PA, USA). Statistical significance between two groups was examined by the unpaired *t*-test. Statistical significance was accepted for $P < 0{\cdot}05$.

Results

Procoagulant alteration of PNH RBC by C′ activation

IIa generation in the diluted plasma by the addition of Ca^{2+} was measured in the presence of RBC. In the presence of PNH RBC that were C′ activated in sucrose buffer, IIa generation was enhanced in comparison with normal RBC treated similarly or under cell-free conditions (Fig 2A). Such procoagulant alteration of PNH RBC was reversed by the subsequent treatment of PNH RBC with Annexin V, which binds to the PS exposed on RBC (Fig 2B).

Release of procoagulant MPs from C′-activated PNH RBC

The IIa-generation assay used in the present study, showed a linear correlation between time (0–60 min) and OD_{405} of IIa at 0–60 u/l, added to the wells (Fig 1A). The procoagulant properties of the supernatants of RBC (normal and PNH) treated by C′ activation in sucrose buffer were examined by acceleration of the IIa-generation process in the diluted plasma. The supernatants of PNH RBC, which were treated by C′ activation, showed enhanced procoagulant properties in comparison with those of normal RBC similarly treated or PNH RBC treated with inactivated serum (Fig 1B). Both supernatants of normal RBC treated with serum and PNH-RBC treated with inactivated serum in sucrose buffer showed enhanced procoagulant properties, suggesting that some components included in the serum may accelerate coagulation.

To measure procoagulant MPs in the supernatants, we also employed a ZYUMUPHEN-MP Activity kit, which is based upon PS-exposed MPs captured in Annexin V-coated wells accelerating the action of prothrombinase added to the wells. C′ activation induced the release of significant amounts of MPs from PNH RBC but not from normal RBC; interruption of terminal C′ activation with anti-C5 or anti-C9 inhibited MP release from PNH RBC (Fig 3).

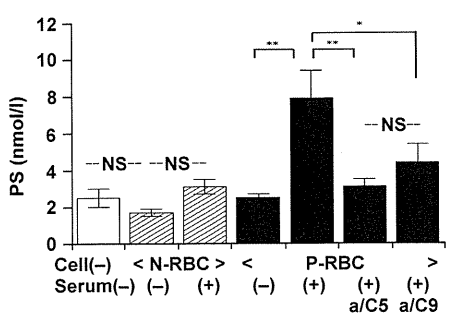

Fig 3. PS-exposed (procoagulant) MP release from RBC by C′-activation. Annexin V binding, i.e. PS-exposed MPs released from RBC by C′ activation was measured using a procoagulant MP Activity Assay kit. C′ activation induced significant amounts of PS-exposed MPs released from PNH-RBC (P-RBC), but not from normal RBC (N-RBC). Interruption of C′ activation with anti-C5 (a/C5) or anti-C9 (a/C9) inhibited the release of MPs from PNH-RBC. This figure shows data for Patient 2. Bars indicate the mean ± SD of triplicate assays. NS, not significant. $*P < 0{\cdot}05$; $**P < 0{\cdot}01$.

FCM for MP release and PS exposure on RBC

FCM detects MPs as low forward scatter (FSC-low) and Annexin V-binding regions. While no significant MPs were generated from normal RBC by C′ activation (Fig 4Ab), significant amounts of MPs were released from PNH-RBC by C′ activation (26·4% in Fig 4Ae). FCM also detected a significant population of PS-exposing RBC (3·3%) that bound to Annexin V (Fig 4Ae). PNH-RBC were composed of CD59-negative and -positive RBC (a and b, respectively, lower panel in Fig 4B). As expected, only CD59-negative (PNH-affected, i.e. C′-sensitive) RBC released MPs by C′ activation (Fig 4B).

PMA- and C′-induced release of procoagulant MPs from RBC

Procoagulant MPs were released from RBC (both normal and PNH) by treatment with PMA, a PKC activator (Fig 5A,B; ●). This release was inhibited by the pretreatment of RBC with Calphostin C (Fig 5A,B; ■). By contrast, the release of procoagulant MPs from C′-activated PNH RBC was not influenced by the pretreatment of RBC with Calphostin C (Fig 5C).

Effects of PKC inhibitors on C′-induced MP release from PNH RBC

A previous report indicated that PKC activation is involved in PS exposure on RBC induced by calcium and ionophore (de Jong *et al*, 2002), although this was unclear in MP generation from RBC. Our study revealed that PKC activation of RBC (normal RBC as well as PNH-RBC) with PMA enhanced the procoagulant properties of the supernatant of RBC that were inhibited by the pretreatment of RBC with Calphostin C, a blocker of the PMA binding site (Fig 5A,B). As MP generation and PS exposure on RBC are considered to occur in the same phase, we studied the role of PKC in MP generation from PNH-RBC by C′ activation. Procoagulant properties of the supernatants of C′-activated PNH-RBC were not influenced by the pretreatment of PNH-RBC with Calphostin C (Fig 5C). To confirm this phenotypically, the release of Annexin V-binding MPs from PNH-RBC by C′ activation was examined by FCM. Neither Calphostin C nor

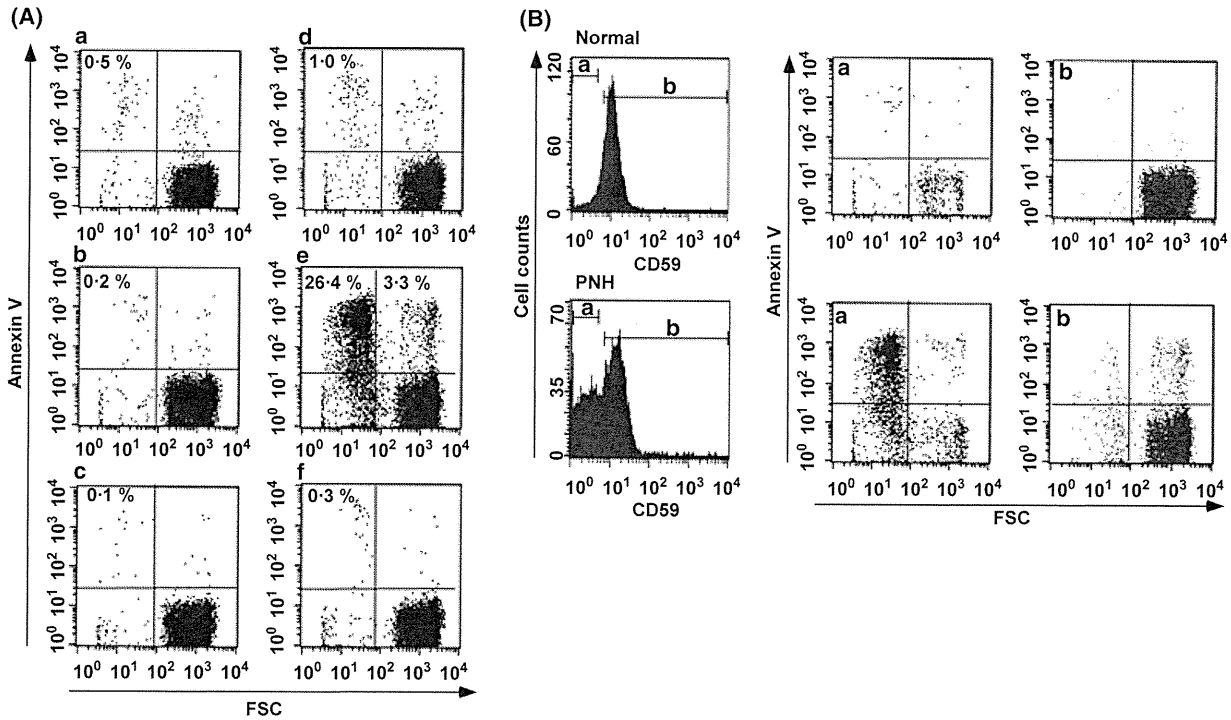

Fig 4. FCM for procoagulant MP release and PS-exposed RBC by C' activation. Panel A: Normal RBC (a,b,c) and PNH-RBC (d,e,f) were incubated with serum (b,e), inactivated serum (c,f), or normal saline (a,d) in sucrose buffer. MPs (FSC-low and Annexin V-high) were detected only when PNH-RBC were treated with serum in sucrose buffer (26·4% in Fig 4Ae). It should be noted that a significant population of PS-exposed RBC was also detected in PNH-RBC treated by C' activation (3·3% in Fig 4Ae). Figures in each panel denote the percentages of the regions with MP or PS-exposed RBC, detected as FSC-low, Annexin V-high or FSC-high, Annexin V-high, respectively. Panel B: PNH phenotype of RBC inducing MP release was analysed by two-colour FCM (FITC-Annexin-V and phycoerythrin-anti-CD59). MPs were shown to be derived from CD59-negative (PNH-affected) RBC (a fraction in lower panel B). CD59-positive, PNH-unaffected RBC were resistant to both MP release and haemolysis upon C' activation (b fraction in lower panel B). This figure shows data for Patient 1.

Ro-31-8220, both PKC inhibitors, affected MP release from C'-activated PNH-RBC in comparison with the controls, distilled water (DDW) or dimethyl sulfoxide (DMSO), respectively (Fig 6).

Involvement of calpain or caspase and Ca^{2+} dependency in C'-induced MP release from PNH-RBC

In the case of activated platelets, it has been reported that PS exposure is regulated by various molecules, such as calpain (calcium-dependent thiol proteinase) or caspase (apoptosis-related protein), although this has not been studied well in RBC. We have studied the role of these molecules in MP generation from PNH-RBC by C' activation using several inhibitors: calpain inhibitors (ALL, E64d, PD150606, PD145305, calpastatin peptide) and a caspase inhibitor [Z–Val–Ala–DL–Asp–fluoromethylketone (z–VAD–fmk)]. These inhibitors did not affect MP release from PNH-RBC (Fig 7A).

In addition, we examined the requirement of Ca^{2+} for MP release from C'-activated PNH-RBC. In sucrose buffer containing 1 mmol/l Mg^{2+}, EGTA did not affect either haemolysis or MP generation from PNH-RBC (Fig 7B). This explains why EDTA (2 mmol/l) blocked both C'-mediated haemolysis and MP release, because EDTA inhibits the assembly of C' membrane attack complex (MAC) on RBC (Fig 7B).

Discussion

Increased incidence of thrombosis has been reported in haemolytic anaemias, particularly anaemias with intravascular haemolytic features, which include sickle cell disease (SCD), thalassaemia and PNH (Cappellini *et al*, 2000; Ataga & Orringer, 2003; Ziakas *et al*, 2008). Pathophysiological mechanisms contributing to coagulation abnormalities in haemolytic anaemias could be classified three ways: (i) RBC membrane alteration and MPs, (ii) RBC/endothelium interaction, (iii) nitric oxide (NO) deficiency (Cappellini, 2007). Although diverse PNH abnormalities in multi-lineages of blood cells, deficient in the expression of GPI-anchored membrane proteins, may contribute to thrombogenesis, the effectiveness of eculizumab (anti-C5) on the reduction of thrombotic incidence as well as the reduction of clinical

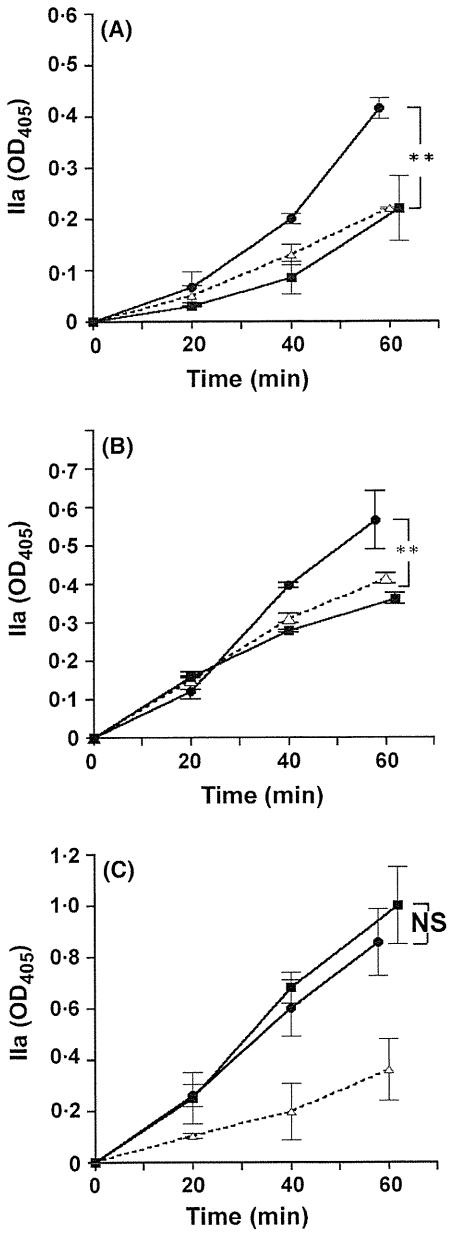

Fig 5. PMA- and C'-induced procoagulant MPs release from RBC. Panel A,B: PMA-induced procoagulant MP release from RBC. The supernatant of normal RBC (A) and PNH-RBC (B), which were treated with PMA (0·1 μmol/l, 30 min), showed enhanced procoagulant properties (black circle) in comparison with those of untreated RBC (open triangle). The supernatant of RBC, pretreated RBC with Calphostin C (1·67 μmol/l, 30 min) followed by treatment with PMA, showed no enhancement of procoagulant properties (black square). There were no differences in PMA-induced MP release between normal and PNH-RBC. This figure shows data for a normal donor (A) and for Patient No.1 (B). Panel C: Effects of Calphostin C on MP release from C'-activated PNH-RBC. Both supernatants of PNH-RBC pretreated with (black square) or without (black circle) Calphostin C followed by C'-activation showed enhanced procoagulant properties. Data of untreated RBC are shown as open triangles. Bars indicate the mean ± SD of triplicate assays. NS, not significant. $^{**}P < 0{\cdot}01$. This figure shows data for Patient 2.

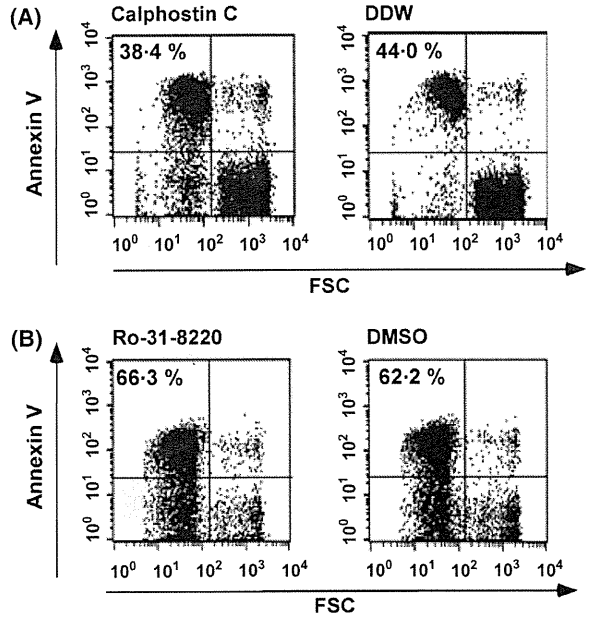

Fig 6. PKC activation is not involved in MP release from C'-activated PNH-RBC. PNH-RBC were pretreated with PKC inhibitors, Calphostin C or Ro-31-8220, followed by C' activation. MP release was analysed by FCM. Panel A: Pretreatment of PNH-RBC (Patient 1) with Calphostin C (10 μmol/l, 23°C, 30 min) did not inhibit MP release from C'-activated PNH-RBC in comparison with the control (double-distilled water, DDW). Panel B: Pretreatment of PNH-RBC (Patient 2) with Ro-31-8220 (100 nmol/l, 23°C, 30 min) did not inhibit MP release from C'-activated PNH-RBC in comparison with the control (dimethyl sulfoxide, DMSO). Figures in each panel denote the percentages of regions of MPs (FSC-low, Annexin V-high). Panels (A) and (B) show data for Patients 1 and 2, respectively.

haemolysis (Hillmen *et al*, 2004, 2007) indicate the importance of C'-mediated mechanisms, haemolysis in particular, for thrombogenesis in PNH. As has been well documented for platelets, cell membrane-derived MPs provide the catalytic surface necessary for the assembly of procoagulant enzyme complexes, prothrombinase and tenase. In PNH, the increased levels of circulating procoagulant MPs, derived from haemolysed RBC or activated platelets, could be responsible for the prothrombotic status (Hugel *et al*, 1999; Simak *et al*, 2004), as well as in sepsis, heparin-induced thrombocytopenia, thrombotic thrombocytopenic purpura and SCD (Piccin *et al*, 2007). While elevated levels of circulating MPs could contribute to the thrombophilia in PNH, their precise correlation with the thrombotic events in PNH remains to be clarified. Because NO plays an important role in the maintenance of normal platelet functions through the downregulation of platelet aggregation and adhesion, NO reduction due to intravascular haemolysis also contributes to thrombogenesis in PNH to some extent (Cappellini, 2007). In addition, the effects of eculizumab on the clinical markers of coagulation and fibrinolysis indicate that endothelial cell activation also plays some role(s) in thrombogenesis in PNH (Helley *et al*, 2009).

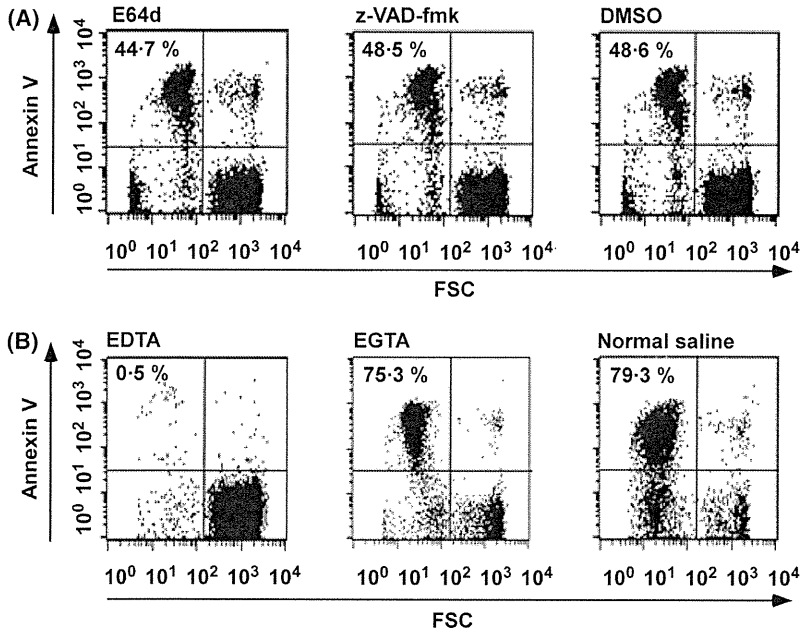

Fig 7. Panel (A): Effects of calpain and caspase inhibitor on C'-induced MPs release from PNH-RBC. Pretreatment of PNH-RBC (Patient 1) with E64d (40 μmol/l, 23°C, 15 min), a calpain inhibitor, or with z-VAD-fmk (100 μmol/l, 23°C, 15 min), a broad caspase inhibitor, did not influence MP release from PNH-RBC by C' activation. DMSO indicates the control. Calpain inhibitors other than E64d showed the same results. Panel (B): Effects of chelating agents on C'-induced MP release from PNH-RBC. C' activation of PNH-RBC (Patient 2) was induced in the presence of EDTA (2 mmol/l), EGTA (2 mmol/l), or normal saline (control) in sucrose buffer containing 1 mmol/l $MgCl_2$. EDTA inhibited both haemolysis and MP release. EGTA and haemolysis did not affect MP release from PNH-RBC. Figures in each panel denote the percentages of regions of MPs (FSC-low, Annexin V-high).

Mammalian cells have an asymmetric transbilayer distribution of phospholipids, in which most PS is located in the inner monolayer. This asymmetry is maintained by the activity of a lipid-specific transporter that regulates the distribution of PS between bilayer leaflets, a process that is Ca^{2+}-dependent (Sims & Wiedmer, 2001). It has been well established that PS exposure is regulated by activation of calcium-dependent phospholipid scramblase activity in concert with inactivation of the aminophospholipid translocase. MP release, generally accompanied by the loss of transversal phospholipid asymmetry leading to PS exposure, occurs during cell ageing and in disease states (Allan *et al*, 1982) or in *in vitro* conditions as the increase of intracellular Ca^{2+} induced by an ionophore (Allan & Thomas, 1981).

PS exposure and/or procoagulant MP generation in RBC can be induced by various mechanisms, such as intracellular calcium increase (Dekkers *et al*, 1998), PKC activation (de Jong *et al*, 2002) and ATP depletion (Beleznay *et al*, 1997); C5b-9 deposition on cell membranes is one such mechanism, in RBC as well as platelets (Wiedmer *et al*, 1993; Ninomiya *et al*, 1999). Our study demonstrated that the accumulation of C' MAC on RBC induces procoagulant MP release, which was shown both functionally by IIa generation assay and phenotypically by FCM. The data that the treatment of serum (source of C') with anti-C9 significantly diminished MP generation from PNH-RBC upon C' activation indicate that PS exposure and MP release are not induced significantly before the step of C5b-8 MAC formation. While PNH-RBC, deficient in the expression of GPI-anchored proteins, including CD55 and CD59, have been shown to be impaired in MP release in response to Ca^{2+} ionophore stimulation (Whitlow *et al*, 1993), our data showed that PNH-RBC release MPs in response to C5b-9 accumulation in a Ca^{2+}-independent manner; normal RBC expressing GPI-anchored proteins were resistant to PS exposure and MP release in response to C' activation, as clearly shown in Fig 4. Normal RBC are resistant to C' activation inducing the assembly of C5b-9 MAC leading to haemolysis and MPs release, because of the normal expression of membrane C' inhibitors, CD55 and CD59.

It is known that human RBC contain PKC, which mediates the phosphorylation of cytoskeletal proteins (Danilov & Cohen, 1989) and the human Na^+/H^+ antiport (Bourikas *et al*, 2003). PKCα, which translocates to the RBC membrane upon stimulation with PMA, mediates PS exposure following glucose depletion of RBC (Klarl *et al*, 2006). In the case of platelet activation accompanied by MP release in response to calcium ionophore, the involvement of calpain-mediated proteolysis of cytoskeletal proteins was also suggested (Fox *et al*, 1990), but not in the response to C5b-9 (Wiedmer *et al*, 1990). Our data indicated that PKC, calpain and caspase were not involved in MP release from RBC by terminal C' MAC accumulation. This finding is also consistent with MP release from PNH RBC by C' activation being Ca^{2+}-independent.

Although the precise mechanism underlying PS exposure and/or procoagulant MP release from PNH-RBC by C′ stimulation is still to be clarified, procoagulant MPs derived from PNH-affected blood cells could contribute to thrombogenesis in PNH, in addition to other pathophysiological mechanisms, particularly due to activated platelets and/or injured endothelial cells. To clarify the precise contribution of elevated MPs derived from PNH-RBC to the thrombogenesis in PNH, a clinical study in a large scale, further studies on the MPs in PNH patients are required.

References

Allan, D. & Thomas, P. (1981) Ca^{2+}-induced biochemical changes in human erythrocytes and their relation to microvesiculation. *Biochemical Journal*, **198,** 433–440.

Allan, D., Limbrick, A.R., Thomas, P. & Westerman, M.P. (1982) Release of spectrin-free spicules on reoxygenation of sickled erythrocytes. *Nature*, **295,** 612–613.

Andrews, D.A., Yang, L. & Low, P.S. (2002) Phorbol ester stimulates a protein kinase C-mediated agatoxin-TK-sensitive calcium permeability pathway in human red blood cells. *Blood*, **100,** 3392–3399.

Ataga, A.I. & Orringer, E.P. (2003) Hypercoagulability in sickle cell disease: a curious paradox. *American Journal of Medicine*, **115,** 721–728.

Bachelot-Loza, C., Badol, P., Brohard-Bohn, B., Fraiz, N., Cano, E. & Rendu, F. (2006) Differential regulation of platelet aggregation and aminophospholipid exposure by calpain. *British Journal of Haematology*, **133,** 419–426.

Beleznay, Z., Zachowski, A., Devaux, P.F. & Ott, P. (1997) Characterization of the correlation between ATP-dependent aminophospholipid translocation and Mg^{2+}-ATPase activity in red blood cell membranes. *European Journal of Biochemistry*, **243,** 58–65.

Bourikas, D., Kaloyianni, M., Bougoulia, M., Zolota, Z. & Koliakos, G. (2003) Modulation of the Na^{+}–H^{+} antiport activity by adrenaline on erythrocytes from normal and obese individuals. *Molecular and Cellular Endocrinology*, **205,** 141–150.

Brodsky, R.A. (2008) Advances in the diagnosis and therapy of paroxysmal nocturnal hemoglobinuria. *Blood Reviews*, **22,** 65–74.

Bucki, R., Bachelot-Loza, C., Zachowski, A., Giraud, F. & Sulpice, J.C. (1998) Calcium induces phospholipid redistribution and microvesicle release in human erythrocyte membranes by independent pathways. *Biochemistry*, **37,** 15383–15391.

Cappellini, M.D. (2007) Coagulation in the pathophyiology of hemolytic anemias. *Hematology 2007 American Society of Hematology Education Program Book*, **2007,** 74–78.

Cappellini, M.D., Robbiolo, L., Bottasso, B.M., Coppola, R., Fiorelli, G. & Mannucci, P.M. (2000) Venous thromboembolism and hypercoagulability in splenectomized patients with thalassaemia intermedia. *British Journal of Haematology*, **111,** 467–473.

Danilov, Y.N. & Cohen, C.M. (1989) Wheat germ agglutinin but not concanavalin A modulates protein kinase C-mediated phosphorylation of red cell skeletal proteins. *FEBS Letters*, **257,** 431–434.

Dekkers, D.W.C., Comfurius, P., Vuist, W.M.J., Billheimer, J.T., Dicker, I., Weiss, H.J., Zwaal, R.F.A. & Bevers, E.M. (1998) Impaired Ca^{2+}-induced tyrosine phosphorylation and defecetive lipid scrambling in erythrocytes from a patient with Scott syndrome: a study using an inhibitor for scramblase that mimics the defect in Scott syndrome. *Blood*, **91,** 2133–2138.

Devaux, P.F. (1991) Static and dynamic lipid asymmetry in cell membranes. *Biochemistry*, **30,** 1163–1173.

Fox, J.E.B., Austin, C.D., Boyles, J.K. & Steffen, K. (1990) Role of the membrane skeleton in preventing the shedding of procoagulant-rich microvesicles from platelet plasma membrane. *Journal of Cellular Biology*, **111,** 483–493.

Helley, D., de Latour, R.P., Porcher, R., Rodrigues, C.A., Galy-Fauroux, I., Matheron, J., Duval, A., Schved, J.-F., Fischer, A.-M. & Socie, G. (2010) Evaluation of hemostasis and endothelial function in patients with paroxysmal nocturnal hemoglobinuria receiving eculizumab. *Hematologica*, **95,** 574–581.

Hillmen, P., Hall, C., Marsch, J.C.W., Elebute, M., Bombara, M.P., Petro, B.E., Cullen, M.J., Richards, S.J., Rollins, S.A., Mojcik, C.F. & Rother, R.P. (2004) Effect of eculizumab on hemolysis and transfusion requirements in patients with paroxysmal nocturnal hemoglobinuria. *New England Journal of Medicine*, **350,** 552–559.

Hillmen, P., Muus, P., Dührsen, U., Risitano, A.M., Schubert, J., Luzzatto, L., Schrezenmeier, H., Szer, J., Brodsky, R.A., Hill, A., Socié, G., Bessler, M., Rollins, S.A., Bell, L., Rother, R.P. & Young, N.S. (2007) Effect of the complement inhibitor eculizumab on thromboembolism in patients with paroxysmal nocturnal hemoglobinuria. *Blood*, **110,** 4123–4128.

Hugel, B., Socie, G., Vu, T., Toti, F., Gluckman, E., Freyssinet, J.M. & Scrobohaci, M.L. (1999) Elevated levels of circulating procoagulant microparticles in patients with paroxysmal nocturnal hemoglobinuria and aplastic anemia. *Blood*, **93,** 3451–3456.

de Jong, K., Rettig, M.P., Low, P.S. & Kuypers, F.A. (2002) Protein kinase C activation induces phosphatidylserine exposure on red blood cells. *Biochemistry*, **41,** 12562–12567.

Kamp, D., Sieberg, T. & Haest, C.W.M. (2001) Inhibition and stimulation of phospholipid scrambling activity. Consequences for lipid asymmetry, echinocytosis, and microvesiculation of erythrocytes. *Biochemistry*, **40,** 9438–9446.

Klarl, B.A., Lang, P.A., Kempe, D.S., Niemoeller, O.M., Akel, A., Sobiesiak, M., Eisele, K., Podolski, M., Huber, S.M., Wieder, T. & Lang, F. (2006) Protein kinase C mediates erythrocyte "programmed cell death" following glucose depletion. *American Journal of Physiology and Cellular Physiology*, **290,** C244–C253.

Ninomiya, H., Kawashima, Y., Hasegawa, Y. & Nagasawa, T. (1999) Complement-induced procoagulant alteration of red blood cell membranes with microvesicle formation in paroxysmal nocturnal haemoglobinuria (PNH): implication for thrombogenesis in PNH. *British Journal of Haematology*, **106,** 224–231.

Parker, C., Omine, M., Richards, S., Nishimura, J., Bessler, M., Ware, R., Hillmen, P., Luzzatto, L., Young, N., Kinoshita, T., Rosse, W. & Socié, G. & International PNH Interest Group (2005) Diagnosis and management of paroxysmal nocturnal hemoglobinuria. *Blood*, **106,** 3699–3709.

Piccin, A., Murphy, W.G. & Smith, O.P. (2007) Circulating microparticles: pathophysiology and clinical implications. *Blood Reviews*, **21,** 157–171.

Ploug, M., Plesner, T., Rønne, E., Ellis, V., Høyer-Hansen, G., Hansen, N.E. & Danø, K. (1992) The receptor for urokinase-type plasminogen activator is deficient on peripheral blood leukocytes in patients with paroxysmal nocturnal hemoglobinuria. *Blood*, **79,** 1447–1455.

Seigneuret, M. & Devaux, P.F. (1984) ATP-dependent asymmetric distribution of spin-labeled phospholipids in the erythrocyte membrane: relation to shape changes. *Proceedings of the National Academy of Sciences of the United States of America*, **81,** 3751–3755.

Shcherbina, A. & Remold-O'Donnell, E. (1999) Role of caspase in a subset of human platelet activation responses. *Blood*, **93,** 4222–4231.

Simak, J., Holada, K., Risitano, A.M., Zivny, J.H., Young, N.S. & Vostal, J.G. (2004) Elevated circulating endothelial membrane microparticles in paroxysmal nocturnal haemoglobinuria. *British Journal of Haematology*, **125,** 804–813.

Sims, P.J. & Wiedmer, T. (2001) Unraveling the mysteries of phospholipid scrambling. *Thrombosis and Haemostasis*, **86,** 266–275.

Whitlow, M., Iida, K., Marshall, P., Silber, R. & Nussenzweig, V. (1993) Cells lacking glycan phosphatidylinositol-linked proteins have impaired ability to vesiculate. *Blood*, **81,** 510–516.

Wiedmer, T., Shattil, S.J., Cunningham, M. & Sims, P.J. (1990) Role of calcium and calpain in complement induced vesiculation of the platelet plasma membrane and in the exposure of the platelet factor Va receptor. *Biochemistry*, **29,** 623–632.

Wiedmer, T., Hall, S.E., Ortel, T.L., Kane, W.H., Rosse, W.F. & Sims, P.J. (1993) Complement-induced vesiculation and exposure of membrane prothrombinase sites in platelets of

paroxysmal nocturnal hemoglobinuria. *Blood*, **82,** 1192–1196.

Wilcox, L.A., Ezzell, J.L., Bernshaw, N.J. & Parker, C.J. (1991) Molecular basis of the enhanced susceptibility of the erythrocytes of paroxysmal nocturnal hemoglobinuria to hemolysis in acidified serum. *Blood*, **78,** 820–829.

Zhou, Q., Zhao, J., Stout, J.G., Luhm, R.A., Wiedmer, T. & Sims, P.J. (1997) Molecular cloning of human plasma membrane phospholipids scramblase. A protein mediating transbilayer movement of plasma membrane phospholipids. *Journal of Biological Chemistry*, **272,** 18240–18244.

Ziakas, P.D., Poulou, L.S. & Pomoni, A. (2008) Thrombosis in paroxysmal nocturnal hemoglobinuria at a glance: a clinical review. *Current Vascular Pharmacology*, **6,** 347–353.

blood

2011 118: 1374-1385
Prepublished online May 31, 2011;
doi:10.1182/blood-2010-08-300400

c-Maf plays a crucial role for the definitive erythropoiesis that accompanies erythroblastic island formation in the fetal liver

Manabu Kusakabe, Kazuteru Hasegawa, Michito Hamada, Megumi Nakamura, Takayuki Ohsumi, Hirona Suzuki, Tran Thi Nhu Mai, Takashi Kudo, Kazuhiko Uchida, Haruhiko Ninomiya, Shigeru Chiba and Satoru Takahashi

Blood (print ISSN 0006-4971, online ISSN 1528-0020), is published weekly by the American Society of Hematology, 2021 L St, NW, Suite 900, Washington DC 20036.

c-Maf plays a crucial role for the definitive erythropoiesis that accompanies erythroblastic island formation in the fetal liver

Manabu Kusakabe,[1,2] Kazuteru Hasegawa,[1] Michito Hamada,[1] Megumi Nakamura,[1] Takayuki Ohsumi,[1] Hirona Suzuki,[1] Mai Thi Nhu Tran,[3] Takashi Kudo,[1] Kazuhiko Uchida,[4] Haruhiko Ninomiya,[2] Shigeru Chiba,[2] and Satoru Takahashi[1]

[1]Department of Anatomy and Embryology, Institute of Basic Medical Sciences, and [2]Department of Hematology, Institute of Clinical Medicine, Graduate School of Comprehensive Human Sciences, University of Tsukuba, Tsukuba, Ibaraki, Japan; [3]Laboratory of Stem Cell Research and Application, University of Science, Ho Chi Minh City, Vietnam; and [4]Department of Molecular Biological Oncology, Institute of Basic Medical Sciences, Graduate School of Comprehensive Human Sciences, University of Tsukuba, Tsukuba, Ibaraki, Japan

c-Maf is one of the large Maf (musculoaponeurotic fibrosarcoma) transcription factors that belong to the activated protein-1 super family of basic leucine zipper proteins. Despite its overexpression in hematologic malignancies, the physiologic roles c-Maf plays in normal hematopoiesis have been largely unexplored. On a C57BL/6J background, *c-Maf*$^{-/-}$ embryos succumbed from severe erythropenia between embryonic day (E) 15 and E18. Flow cytometric analysis of fetal liver cells showed that the mature erythroid compartments were significantly reduced in *c-Maf*$^{-/-}$ embryos compared with *c-Maf*$^{+/+}$ littermates. Interestingly, the CFU assay indicated there was no significant difference between *c-Maf*$^{+/+}$ and *c-Maf*$^{-/-}$ fetal liver cells in erythroid colony counts. This result indicated that impaired definitive erythropoiesis in *c-Maf*$^{-/-}$ embryos is because of a non–cell-autonomous effect, suggesting a defective erythropoietic microenvironment in the fetal liver. As expected, the number of erythroblasts surrounding the macrophages in erythroblastic islands was significantly reduced in *c-Maf*$^{-/-}$ embryos. Moreover, decreased expression of VCAM-1 was observed in *c-Maf*$^{-/-}$ fetal liver macrophages. In conclusion, these results strongly suggest that c-Maf is crucial for definitive erythropoiesis in fetal liver, playing an important role in macrophages that constitute erythroblastic islands. (*Blood*. 2011;118(5): 1374-1385)

Introduction

In mouse embryogenesis, red blood cells are produced in the yolk sac in a process called primitive erythropoiesis. Erythropoiesis then takes place in the fetal liver around embryonic day (E) 10 onward and in BM and spleen after birth. This process, which is characterized by enucleated red blood cells, is called definitive erythropoiesis.[1] During terminal erythroid differentiation, erythroblasts are associated with a central macrophage, which forms a specialized microenvironment, the so-called erythroblastic islands. In the erythroblastic islands, a central macrophage provides favorable proliferative and survival signals to the surrounding erythroblasts, and it eventually engulfs the extruded nuclei of maturing erythrocytes.[2-5] Inhibition of the interaction between macrophage and erythroblasts usually leads to embryonic anemia accompanied by accelerated apoptosis of erythroid cells. Targeted disruption of the gene *palld*, which encodes actin cytoskeleton associated protein (palladin) prevented effective erythroblast-macrophage interactions because of differentiation defects in the macrophage. Therefore, mouse embryos homozygous for the mutant gene experience severe anemia and succumb in the embryonic period.[6] Meanwhile, it has been reported that a series of adhesion molecules are also involved in the process of forming erythroblastic islands. Erythroblast macrophage protein (EMP) is a transmembrane protein expressed in both erythroblasts and macrophages, and it mediates the erythroblast-macrophage interaction. Indeed, the targeted deletion of EMP causes lethal anemia in mouse embryos because of the suppressed formation of erythroblastic islands.[7] Furthermore, a previous report showed that the interaction between very late Ag-4 ($\alpha_4\beta_1$ integrin) on erythroblasts and VCAM-1 on macrophages plays a key role in maintaining the islands.[8] For example, administration of Abs raised against either $\alpha_4\beta_1$ integrin or VCAM-1 caused disruption of the island structure.[8] However, the molecular mechanism, in terms of transcriptional regulation of island-affiliated genes in macrophages, remains largely unknown.

The large Maf transcription factor c-Maf is a cellular homolog of v-maf, which was isolated from a chicken musculoaponeurotic fibrosarcoma induced by avian retrovirus AS42 infection.[9] The large Maf transcription factors contain an acidic domain that promotes transcriptional regulation and a basic region/leucine zipper domain that mediates dimerization, as well as DNA binding to either Maf recognition elements (MAREs) or the 5′ AT-rich half-MARE.[10-12] Each large Maf protein has been shown to play a distinct role in cellular proliferation and differentiation in both pathologic and physiologic situations.[9,13-19] In B-lymphoid and T-lymphoid lineages, aberrant expression of c-Maf works as an oncogene, as shown in patients with multiple myeloma and angioimmunoblastic T-cell lymphoma and in a transgenic mouse model.[20-23] Physiologic c-Maf expression is indispensable for the proper regulation of IL-4 and IL-21 gene expression in T-helper cells.[24,25] In macrophages, c-Maf has been reported to regulate IL-10 expression, which is essential for differentiation of regulatory T cells.[26] In addition, combined deficiency of MafB and c-Maf

Submitted August 4, 2010; accepted May 3, 2011. Prepublished online as *Blood* First Edition paper, May 31, 2011; DOI 10.1182/blood-2010-08-300400.

An Inside *Blood* analysis of this article appears at the front of this issue.

The online version of the article contains a data supplement.

The publication costs of this article were defrayed in part by page charge payment. Therefore, and solely to indicate this fact, this article is hereby marked "advertisement" in accordance with 18 USC section 1734.

enables long-term expansion of differentiated, mature macrophages.[27] We recently reported that c-Maf is abundantly expressed in fetal liver macrophages and that it regulates expression of F4/80, which mediates immune tolerance.[28] However, the physiologic consequences of c-Maf deletion on terminal erythroid differentiation in erythroblastic islands have been largely unexplored.

In the present study, we demonstrate that *c-Maf*–deficient mice exhibit embryonic anemia, which is associated with a failure to retain erythroblastic islands. Moreover, we found significantly reduced expression of VCAM-1 in *c-Maf*–deficient macrophages, which presumably accounts for the deficiency in island maintenance and subsequent embryonic anemia. Thus, these results suggest that c-Maf is indispensable for definitive erythropoiesis in fetal liver, because it activates VCAM-1 expression in macrophages, and this causes the maintenance of erythroblastic islands.

Methods

Mice

c-Maf–deficient mice were originally generated on a 129/Sv background[14] and have been backcrossed onto a C57BL/6J background for > 7 generations. In staging the embryos, gestational day 0.5 (E0.5) was defined as noon of the day a vaginal plug was found after overnight mating. Mice were maintained in specific pathogen-free conditions in a Laboratory Animal Resource Center. All experiments were performed according to the Guide for the Care and Use of Laboratory Animals at the University of Tsukuba.

Hematologic analysis of fetal liver cells, embryonic blood, and adult blood

Single-cell suspensions prepared from fetal livers were washed and resuspended in 1 mL of 2% FBS/PBS. The cell number was counted with the use of a hemocytometer. Collection of embryonic peripheral blood was performed as described previously.[29] Peripheral blood samples from adult mice were obtained from retro-orbital venous plexus with the use of heparin-coated microtubes. Blood counts were determined with an automated hemocytometer (Nihon Kohden). Blood smears were prepared with the wedge technique and were stained with May-Grünwald-Giemsa and then photographed with a Keyence Biorevo BZ-9000 microscope. Images were processed with Photoshop software (Adobe).

Flow cytometry

Freshly isolated fetal liver cells were immunostained at 4°C in PBS/2% FBS in the presence of 5% mouse serum to block Fc receptors. Cells were incubated with FITC-conjugated anti–TER-119 and allophycocyanin (APC)–conjugated anti-CD44 Abs, followed by a 5-minute incubation with phycoerythrin PE-conjugated Annexin V (BioVision) at room temperature. To quantify the presence of VCAM-1 and integrin αV on macrophages, FITC-conjugated anti–Mac-1, Alexa Fluor 647–conjugated anti–VCAM-1 and PE-conjugated anti-integrin αV Abs were used for analyses. All Abs except PE-conjugated annexin V were from eBioscience. Flow cytometry was performed on a Becton Dickinson FACS LSR with CellQuest software. The isolation of erythroblasts at different stages of maturation was performed as described previously.[30] Data were analyzed with FlowJo (Tree Star Inc) analysis software.

Cell cycle analysis

Cell cycle analysis was performed with propidium iodide (PI). Further details are provided in supplemental Methods (available on the *Blood* website; see the Supplemental Materials link at the top of the online article).

Histology and TUNEL assay

Whole E13.5 embryos were fixed in 10% formalin neutral buffer solution (Wako). Paraffin-embedded tissue was sectioned, mounted, and stained with H&E. TUNEL assays were performed with an in situ Apoptosis Detection Kit according to the manufacturer's protocol (TaKaRa). Images were captured by a digital camera system with the use of a Leica DM RXA2 microscope (Leica Microsystems).

CFU assay

CFU assays were performed in MethoCult GF M3434 (StemCell Technologies) for erythroid burst-forming unit (BFU-E) and granulocyte, erythroid, megakaryocyte, and macrophage CFU (CFU-GEMM), and M3334 for erythroid CFU (CFU-E), following the manufacturer's instructions. CFU-E was scored 2 days after plating. BFU-E and CFU-GEMM were scored 8 days after plating.

Preparation of "native" erythroblastic islands and "reconstituted" erythroblastic islands

Native erythroblastic islands were isolated from fetal livers with the use of a previously described protocol.[31] Full details are provided in supplemental Methods.

Microarray analysis of fetal liver macrophages

Microarray analysis was performed as described previously.[32] Further details are provided in supplemental Methods. The data have been deposited in the Gene Expression Omnibus database under the accession number GSE23305.

Real-time RT-PCR analysis of fetal liver macrophages

Macrophages were prepared from fetal livers of *c-Maf*$^{+/+}$ or *c-Maf*$^{-/-}$ mice. Separation of fetal liver macrophages with the use of Mac-1^{+} magnetic beads and the MACS system was performed as described previously.[28] RNA extraction and quantitative RT-PCR were performed as described previously.[28] Primers used for PCR and the PCR conditions are available in supplemental Table 1.

Luciferase reporter assay

The *VCAM-1* 0.7 kilobase (kb) promoter (VCAM-1 Luc) or VCAM-1 mut Luc ligated to a luciferase reporter[33] was transiently cotransfected with c-Maf expression plasmids in macrophage cell line J774 with the use of FuGENE 6 (Roche). Twenty-four hours after the transfection, cells were collected, and reporter gene assays were performed with the Dual Luciferase Kit (Promega). Transfection efficiency was normalized to the expression of *Renilla* luciferase.

Reconstitution of hematopoietic system with fetal liver cells

The donor cells for hematopoietic reconstitution were prepared from E14.5 fetal livers of *c-Maf*$^{+/+}$ or *c-Maf*$^{-/-}$ (C57BL/6J-Ly5.1) mice. Fetal liver cells (2×10^6 cells) were injected into the tail vein of 8- to 10-week-old C57BL/6J-Ly5.2 mice that were previously exposed to x-rays at a 10-Gy dose.

Phenylhydrazine stress test

Mice were injected subcutaneously on days 0, 1, and 3 with 50 mg/kg phenylhydrazine (PHZ) hydrochloride solution in PBS as previously described.[34] Blood was obtained from the retro-orbital plexus on days 0, 3, 6, 8, and 10.

Statistical analysis

Data were represented as mean ± SEM. Statistical significance between any 2 groups was determined by the 2-tailed Student *t* test, in which *P* values < .05 were considered significant.

Table 1. Genotypic analysis of neonates and embryos from *c-Maf*$^{+/-}$ intercross on a C57BL/6J background

Embryonic stage	No. of each *c-Maf* genotype (no. of dead embryos)			Total no. of embryos
	c-Maf$^{+/+}$	*c-Maf*$^{+/-}$	*c-Maf*$^{-/-}$	
E12.5	13	30	15	58
E13.5	57	88	46 (5)	191
E14.5	75	135	55 (12)	265
E15.5	35	58	16 (3)	109
E16.5	11	15	4 (3)	30
E18.5	14	18	4 (3)	36
Neonate	13	29	0	42

Embryos were isolated at the indicated time points of gestation and within 7 days of birth (postnatal), and analyzed for viability. Genotypes of embryos were determined by PCR.

Results

Lethal erythropoietic deficiency in *c-Maf*$^{-/-}$ embryos

The *c-Maf*$^{-/-}$ mice, as originally generated, exhibited perinatal mortality within a few hours after birth on a 129/Sv background.[14] However, unexpectedly, on a C57BL/6J genetic background, c-Maf deficiency resulted in embryonic lethality from E15.5 onward, and almost all *c-Maf*$^{-/-}$ embryos died before E18.5 (Table 1). The fetal livers from *c-Maf*$^{-/-}$ embryos at E13.5 appeared pale compared with those from healthy *c-Maf*$^{+/+}$ control embryos (Figure 1A). As expected, the hematocrits of peripheral blood in the *c-Maf*$^{-/-}$ embryos (E13.5~E15.5) were markedly reduced (E13.5. 13.4% ± 1.8%; E14.5, 14.5% ± 1.0%; E15.5, 16.9% ± 1.0%), compared with the *c-Maf*$^{+/+}$ controls (E13.5, 18.7% ± 0.6%; E14.5, 23.1% ± 1.7%; E15.5, 29.6% ± 1.8%; Figure 1B). May-Grünwald-Giemsa staining of peripheral blood smears showed a significant reduction of enucleated red blood cells in *c-Maf*$^{-/-}$ embryos (E13.5, 6.68% ± 1.0%; E14.5, 17.2% ± 1.9%; E15.5, 29.8% ± 5.6%; Figure 1C-D), whereas *c-Maf*$^{+/+}$ control embryos retained a normal population of enucleated red blood cells (E13.5, 25.5% ± 4.7%; E14.5, 54.1% ± 1.1%; E15.5, 86.9% ± 2.8%; Figure 1C-D). Considering that the enucleated red blood cells are mainly derived from definitive erythropoiesis, these data suggest that c-Maf–deficient embryos suffer from impaired definitive erythropoiesis on the C57BL/6J genetic background. A previous study showed that placental insufficiency causes embryonic lethality.[35] To assess the effect of c-Maf on the placenta, immunofluorescence staining of placenta was performed with an anti–c-Maf Ab (supplemental Figure 1B). The expression of c-Maf was not detected in placenta. Compared with the head tissue as a positive control, c-Maf mRNA expression was 5-fold less in the placenta (supplemental Figure 1C). In addition, no obvious abnormalities in the *c-Maf*$^{-/-}$ placenta were observed after H&E staining (supplemental Figure 1D).

Increased apoptotic cell death in *c-Maf*$^{-/-}$ fetal liver

We next examined the cellular viability, as well as the cell cycle status, of *c-Maf*$^{-/-}$ fetal liver cells, in the hope of elucidating the molecular and cellular basis of their erythropoietic deficiency. The fetal liver size in *c-Maf*$^{-/-}$ embryos was smaller; thus, consistently fewer fetal liver cells were harvested from *c-Maf*$^{-/-}$ embryos between E13.5 and E15.5 (E13.5, 3.37 ± 0.5 × 10^6 cells; E14.5, 7.61 ± 1.0 × 10^6 cells; E15.5, 6.54 ± 2.7 × 10^6 cells) than from age-matched *c-Maf*$^{+/+}$ control embryos (E13.5, 6.89 ± 0.4 × 10^6 cells; E14.5, 16.6 ± 2.3 × 10^6 cells; E15.5, 32.5 ± 2.4 × 10^6 cells; Figure 2A-B). Of note, H&E staining of E13.5 *c-Maf*$^{-/-}$ fetal liver sections showed an increased number of pyknotic nuclei, which are indicative of apoptosis, compared with the *c-Maf*$^{+/-}$ control embryo (Figure 2C). In addition, TUNEL-positive apoptotic cells were remarkably increased in E13.5 *c-Maf*$^{-/-}$ fetal liver sections (Figure 2C). Moreover, flow cytometric analysis of PI-stained fetal liver cells showed an increased abundance of a sub-G_0/G_1 population early apoptotic cell fraction in *c-Maf*$^{-/-}$ fetal liver (8.77% ± 2.5%) compared with *c-Maf*$^{+/+}$

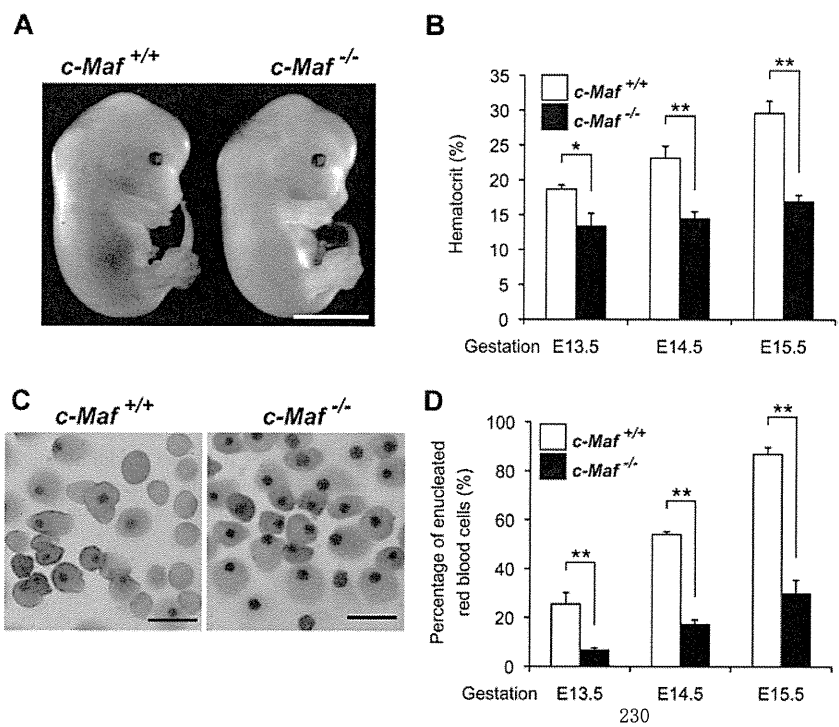

Figure 1. *c-Maf*$^{-/-}$ embryos are anemic. (A) Gross appearance of E13.5 embryos. The *c-Maf*$^{-/-}$ embryo is paler and smaller than its *c-Maf*$^{+/+}$ littermate. Scale bar represents 5 mm. The picture was taken with a NIKON coolpix 5200 digital camera in macro mode and processed with the Adobe Photoshop CS4 software. (B) Hematocrit values for *c-Maf*$^{+/+}$ (n = 6) and *c-Maf*$^{-/-}$ (n = 6) embryos at E13.5, *c-Maf*$^{+/+}$ (n = 8) and *c-Maf*$^{-/-}$ (n = 7) embryos at E14.5, and *c-Maf*$^{+/+}$ (n = 12) and *c-Maf*$^{-/-}$ (n = 9) embryos at E15.5. Data are presented as mean ± SEM. The mean hematocrit values for *c-Maf*$^{-/-}$ embryos were significantly lower than values for *c-Maf*$^{+/+}$ at E13.5, E14.5, and E15.5. (C) Blood smears from E13.5 embryos stained with May-Grünwald-Giemsa stain. The blood smear from a *c-Maf*$^{-/-}$ embryo contains far fewer enucleated red blood cells. Images were acquired by a Biorevo BZ microscope (Plan Apo 20×0.75 DIC N2) at room temperature and processed with the Adobe Photoshop CS4 software. Scale bars represent 20 μm. (D) The percentage of enucleated red blood cells in peripheral blood for *c-Maf*$^{+/+}$ (n = 5) and *c-Maf*$^{-/-}$ (n = 7) embryos at E13.5, *c-Maf*$^{+/+}$ (n = 4) and *c-Maf*$^{-/-}$ (n = 4) embryos at E14.5, and *c-Maf*$^{+/+}$ (n = 8) and *c-Maf*$^{-/-}$ (n = 8) embryos at E15.5. A minimum of 200 cells was counted for each sample. Data are presented as mean ± SEM. The percentage of enucleated red blood cells is significantly reduced in *c-Maf*$^{-/-}$ embryos than in *c-Maf*$^{+/+}$ embryos at E13.5, E14.5, and E15.5. *$P < .05$ and **$P < .01$.

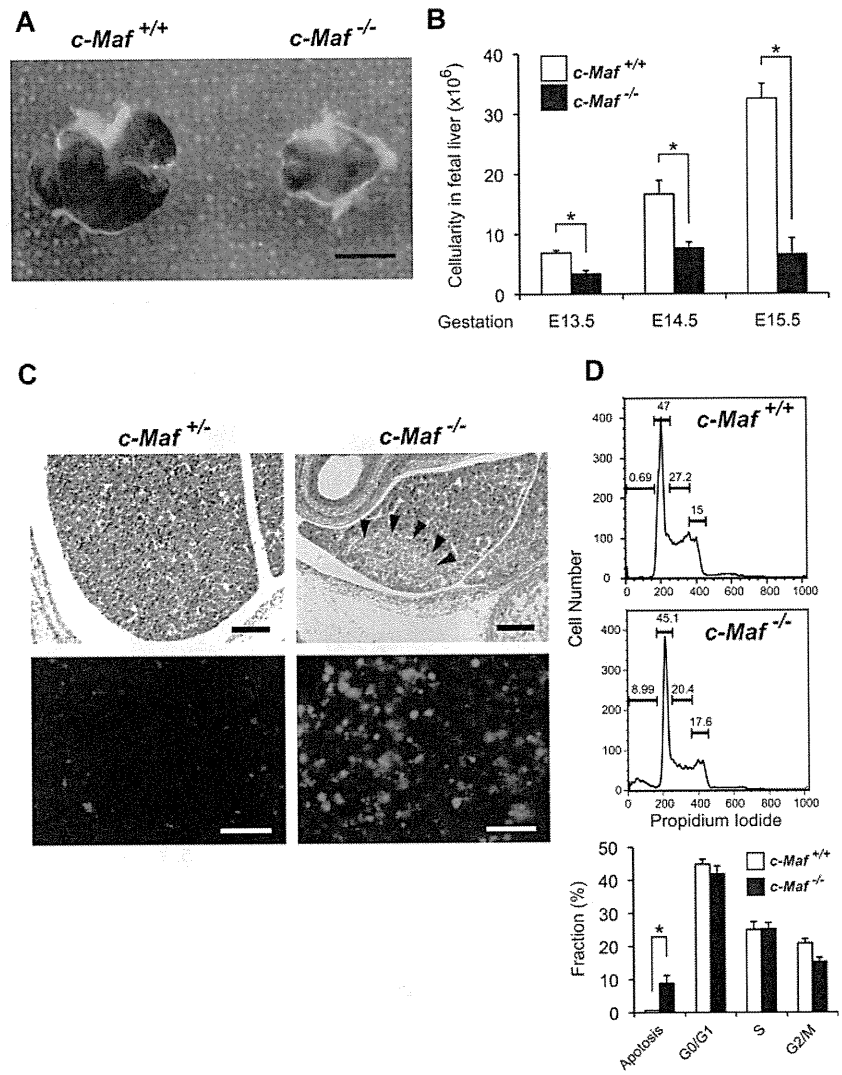

Figure 2. Increased number of apoptotic cells is observed in *c-Maf*$^{-/-}$ fetal liver. (A) Gross appearance of E13.5 fetal liver. The *c-Maf*$^{-/-}$ fetal liver is smaller than a *c-Maf*$^{+/+}$ fetal liver. Scale bar represents 100 μm. The picture was taken with a NIKON coolpix 5200 digital camera in macro mode and processed with the Adobe Photoshop CS4 software.(B) The mean total number of fetal liver cells in *c-Maf*$^{+/+}$ (n = 14) and *c-Maf*$^{-/-}$ (n = 10) embryos at E13.5, *c-Maf*$^{+/+}$ (n = 6) and *c-Maf*$^{-/-}$ (n = 4) embryos at E14.5, and *c-Maf*$^{+/+}$ (n = 8) and *c-Maf*$^{-/-}$ (n = 8) embryos at E15.5. The mean number of fetal liver cells is significantly reduced in *c-Maf*$^{-/-}$ embryos. Data are presented as mean ± SEM. (C) H&D staining of *c-Maf*$^{+/-}$ and *c-Maf*$^{-/-}$ fetal liver sections (top). Arrowheads indicate pyknotic nuclei, which indicate apoptotic cells. TUNEL assays showed increased apoptosis in the *c-Maf*$^{-/-}$ fetal liver (bottom panel). Images were acquired by a Leica DM RXA2 microscope (Lecia HC PL Fluotar 20×/0.50 PH2) at room temperature and processed with the Adobe Photoshop CS4 software. Scale bars in the top panel represent 200 μm. Scale bars in the bottom panel represent 50 μm. (D) The fraction of cells in different phases of the cell cycle was measured by PI staining followed by flow cytometric analyses. The percentage of cells in sub-G_0/G_1, G_1, S phase, and G_2/M are indicated. The sub-G_0/G_1 phase represents the apoptotic population. The apoptotic population was increased in *c-Maf*$^{-/-}$ fetal liver.

control cells (0.67% ± 0.01%; Figure 2D). However, the cellular population of each phase of the cell cycle, that is, G_0/G_1, S, and G_2/M, was not significantly affected (Figure 2D). Overall, these observations suggest that the fetal liver hematopoietic cells from *c-Maf*$^{-/-}$ embryos are prone to undergo apoptotic cell death.

Impaired fetal liver erythropoiesis because of a non–cell-autonomous effect of c-Maf deficiency

Given the significant disturbance of erythropoiesis, we next attempted to delineate the maturation status of erythroid lineage cells in *c-Maf*$^{-/-}$ fetal liver. To this end, we examined fetal liver erythropoiesis by flow cytometry with the use of the erythroid markers CD44 and TER-119, which distinguish various stages of erythroid-cell differentiation (Figure 3A). By modifying a method reported by Chen et al[30] to isolate erythroblasts at different maturation stages from adult BM, we isolated erythroblasts from fetal liver cells and analyzed their structure (Figure 3B). Decreased numbers of mature erythroid compartments (regions II, III, IV, and V in Figure 3C) were observed in *c-Maf*$^{-/-}$ fetal liver than in *c-Maf*$^{+/+}$ fetal liver. These results showed a reduction of basophilic erythroblasts, polychromatic erythroblasts, orthochromatic erythroblasts, reticulocytes, and mature red cells in *c-Maf*$^{-/-}$ fetal liver. Previously, Zhang et al[36] reported a method to study erythropoiesis with the use of an anti-CD71 Ab and an anti–TER-119 Ab. Similar results were obtained with their method. Decreased numbers of mature erythroid compartments (region 3 to region 5 in supplemental Figure 2A-B) were observed in *c-Maf*$^{-/-}$ fetal liver in combination with anti-CD71 Ab and anti–TER-119 Ab. These observations prompted us to quantify the apoptotic cell population at each stage of erythroid cells by annexin V staining.

In good agreement with the preferential decrease of the mature erythroid compartments (regions II-V), we observed a highly increased number of annexin V-positive cells in the most mature erythroid compartment (region V) of *c-Maf*$^{-/-}$ fetal liver compared with the *c-Maf*$^{+/+}$ fetal liver. In contrast, the premature erythroid compartments (regions I-IV) of *c-Maf*$^{-/-}$ fetal liver cells exhibited a comparable number of annexin V-positive cells with the *c-Maf*$^{+/+}$ control (Figure 3D; supplemental Figure 2C). To examine the state of globin regulation, the Mac-1$^-$ cells from E13.5 fetal liver were sorted and analyzed for mRNA of Hbb (hemoglobin beta chain) genes by real-time RT-PCR analysis. Expression profiles showing switching of Hbb genes indicated that the definitive Hbb gene Hbb-b1 (hemoglobin, beta adult major chain) was significantly down-regulated, whereas the primitive globin genes Hbb-bH1

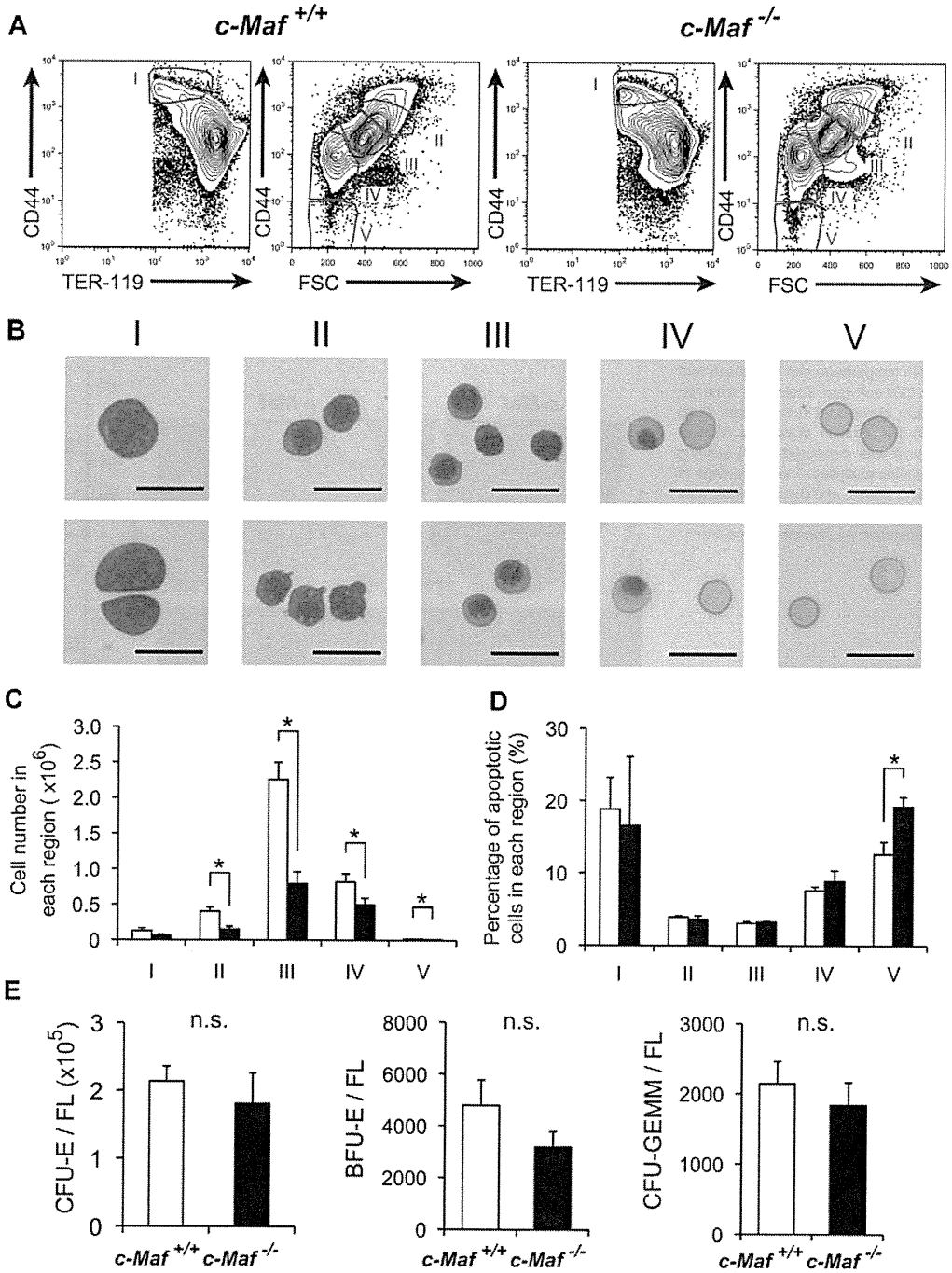

Figure 3. Definitive erythropoiesis in fetal liver is impaired in *c-Maf*$^{-/-}$ embryos but *c-Maf*$^{-/-}$ fetal liver cells can form erythroid colonies. (A) Flow cytometric analysis of fetal liver cells isolated from E13.5 embryos labeled with a FITC-conjugated anti–TER-119 mAb and an APC-conjugated anti-CD44 mAb. Regions I to V are defined by a characteristic staining pattern and forward scatter (FSC) intensity of cells as indicated. (B) Representative images of erythroblast structure on stained cytospins from the 5 distinct regions shown in Figure 3A of wild-type fetal liver. Images were acquired by a Biorevo BZ microscope (Plan Apo 20×0.75 DIC N2) at room temperature and processed with the Adobe Photoshop CS4 software. Scale bar represents 20 μm. (C) Comparison of *c-Maf*$^{+/+}$ and *c-Maf*$^{-/-}$ fetal livers in region I to region V. □ represents *c-Maf*$^{+/+}$; ■, *c-Maf*$^{-/-}$; n = 8~10 per group; **P* < .05. (D) The ratio of annexin V^{+} cells from region I to region V was compared in *c-Maf*$^{+/+}$ and *c-Maf*$^{-/-}$ fetal livers. □ represents *c-Maf*$^{+/+}$; ■, *c-Maf*$^{-/-}$; n = 3 per group; **P* < .05. (E) In vitro colony assay with the use of fetal liver cells from *c-Maf*$^{+/+}$ (□) and *c-Maf*$^{-/-}$ (■) embryos at E13.5. A total of 20 000 fetal liver cells were plated and cultured with methylcellulose media. The numbers of CFU-E–, BFU-E–, and CFU-GEMM–derived colonies per fetal liver are shown. No significant difference (n.s.) was found in the number of CFU-E–, BFU-E–, or CFU-GEMM–derived colonies per fetal liver in *c-Maf*$^{+/+}$ embryos and *c-Maf*$^{-/-}$ embryos; n = 6~7 per group; data are presented as mean ± SEM. FL indicates fetal liver.

(hemoglobin z, beta-like embryonic chain) and Hbb-y (hemoglobin y, beta-like embroyonic chain) were not significantly suppressed in the *c-Maf*$^{-/-}$ fetal liver erythroid fraction compared with the *c-Maf*$^{+/+}$ control (supplemental Figure 3).

To examine the colony formation potential of hematopoietic progenitors in *c-Maf*$^{-/-}$ fetal liver, conventional set of CFU assays were performed. As a result of CFU assays, there were no significant differences between *c-Maf*$^{+/+}$ and *c-Maf*$^{-/-}$ in the

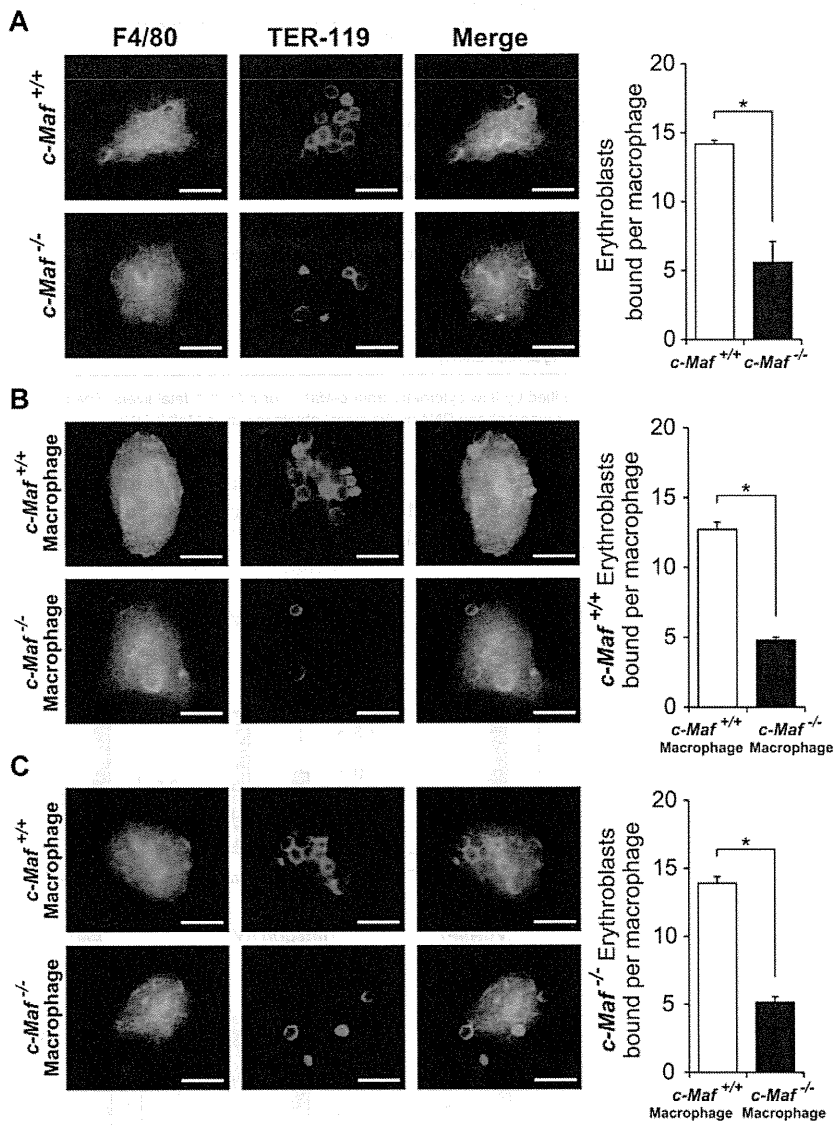

Figure 4. Absence of c-Maf impairs the formation of erythroblastic islands in the fetal liver. (A) Native erythroblastic islands isolated from *c-Maf*$^{+/+}$ and *c-Maf*$^{-/-}$ fetal liver were immunostained with F4/80 (green) and TER-119 (red) Abs as described in "Methods." F4/80 is used as a macrophage-specific marker, and TER-119 is used as a marker for erythroblasts. The number of erythroblasts surrounding each macrophage was significantly reduced in *c-Maf*$^{-/-}$ fetal liver. (B) Erythroblastic islands reconstituted with *c-Maf*$^{+/+}$ erythroblasts were immunostained. The number of *c-Maf*$^{+/+}$ erythroblasts surrounding each *c-Maf*$^{+/+}$ or *c-Maf*$^{-/-}$ macrophage is shown. *c-Maf*$^{+/+}$ erythroblasts surrounding *c-Maf*$^{-/-}$ macrophages were significantly reduced compared with those seen for *c-Maf*$^{+/+}$ macrophages. (C) Erythroblastic islands reconstituted with *c-Maf*$^{-/-}$ erythroblasts were immunostained. The number of *c-Maf*$^{-/-}$ erythroblasts surrounding each *c-Maf*$^{+/+}$ or *c-Maf*$^{-/-}$ macrophage is shown. *c-Maf*$^{-/-}$ erythroblasts surrounding *c-Maf*$^{-/-}$ macrophage were significantly reduced compared with those seen for *c-Maf*$^{+/+}$ macrophages. Although *c-Maf*$^{-/-}$ erythroblasts can form reconstituted erythroblastic islands with *c-Maf*$^{+/+}$ macrophages, *c-Maf*$^{-/-}$ macrophages showed impaired formation of reconstituted erythroblastic islands with *c-Maf*$^{+/+}$ erythroblasts. Images were acquired by a Biorevo BZ microscope (Plan Apo 20×0.75 DIC N2) at room temperature and processed with the Adobe Photoshop CS4 software. The scale bar represents 20 μm; n = 4~6 embryos per group. For each combination, ≥ 20 macrophages per embryo were analyzed. *$P < .05$. Data are presented as mean ± SEM.

number of CFU-E–, BFU-E–, and CFU-GEMM–derived colonies per fetal liver (Figure 3E). In addition, CFU-E colonies were indistinguishable in structure and size (supplemental Figure 4A-B). Moreover, erythroid cells derived from *c-Maf*$^{-/-}$ CFU-Es exhibited a similar structure, and enucleated red blood cells were also similar to those from *c-Maf*$^{+/+}$ control CFU-Es in cytospin slides stained with May-Grünwald-Giemsa (supplemental Figure 4C). Taken together, these results suggest that *c-Maf*$^{-/-}$ erythroid cells are still capable of developing into mature cells in vitro, in contrast to the result of flow cytometric analysis with the use of fetal liver cells (Figures 3A-C; supplemental Figure 2A-B), which reflects the in vivo condition. Therefore, the impaired definitive erythropoiesis in the *c-Maf*$^{-/-}$ embryos is more likely because of a non–cell-autonomous effect of c-Maf deficiency.

Absence of c-Maf causes impaired erythroblastic island formation in the fetal liver

c-Maf is abundantly expressed in fetal liver macrophages, although it is largely missing from the erythroid cells in fetal liver. Therefore, we initially surmised that c-Maf deficiency in fetal liver macrophages disturbed the erythroblastic islands.[3] To address this hypothesis, we attempted to examine whether *c-Maf*$^{-/-}$ macrophages failed to maintain the erythroblastic islands. For this purpose, we isolated the erythroblastic island from *c-Maf*$^{+/+}$ and *c-Maf*$^{-/-}$ fetal livers and counted the number of erythroblasts associated with each single central macrophage according to a previously described method.[31]

Interestingly, although > 10 TER-119^{+} erythroblasts were adhered to a F4/80^{+} macrophage in *c-Maf*$^{+/+}$ fetal livers, c-Maf–deficient central macrophages seemed to harbor far fewer erythroblasts (Figure 4). As shown in Figure 4A, the number of erythroblasts attached to a single central macrophage was significantly reduced in *c-Maf*$^{-/-}$ erythroblastic islands (14.2 ± 0.3 and 5.6 ± 1.5 erythroblasts per macrophage for *c-Maf*$^{+/+}$ and *c-Maf*$^{-/-}$, respectively). This result clearly indicates that erythroblastic islands are impaired in the *c-Maf*$^{-/-}$ fetal livers.

Next, to address whether c-Maf deficiency in macrophages was specifically responsible for the impairment of erythroblastic islands, a series of reconstitution experiments was performed. After attaching native erythroblastic islands either from *c-Maf*$^{+/+}$ or *c-Maf*$^{-/-}$ fetal livers on a glass coverslip, the adherent erythroblasts in the islands were stripped from the macrophages. Next, the

Table 2. Expression of genes comprising the macrophage signature

Symbol	Official full name	*c-Maf*$^{+/+}$ signal	*c-Maf*$^{-/-}$ signal	Fold
VCAM-1	Vascular cell adhesion molecule 1	8.3	1.6	0.19
Mrc1	Mannose receptor, C type 1	19.8	5.7	0.29
Csf1r	Colony stimulating factor 1 receptor	45	16.8	0.37
Sell	Selectin, lymphocyte	26.7	10	0.37
Lamp2	Lysosomal-associated membrane protein 2	8.9	3.3	0.37
Itgav	Integrin α V	1.2	0.5	0.41
Maea (EMP)	Macrophage erythroblast attacher	26.2	14.5	0.55
Emr1 (F4/80)	EGF-like module containing, mucin-like, hormone receptor-like sequence 1	71.4	48.1	0.67
Itgam (Mac-1)	Integrin α M	5.8	3.9	0.67
Cd163	CD163 antigen	0.6	0.4	0.67
Cd14	CD14 antigen	11.8	9.4	0.80
Fcgr1	Fc receptor, IgG, high-affinity I	15.7	17.6	1.12

Fetal liver macrophages were purified by flow cytometry from *c-Maf*$^{+/+}$ or *c-Maf*$^{-/-}$ fetal livers. The fold change in the gene expression was determined by dividing the signal obtained with *c-Maf*$^{-/-}$ fetal liver macrophage RNA by the signal obtained with *c-Maf*$^{+/+}$ RNA.

freshly isolated erythroblasts from *c-Maf*$^{+/+}$ or *c-Maf*$^{-/-}$ fetal livers were cocultured on the remaining adherent *c-Maf*$^{+/+}$ or *c-Maf*$^{-/-}$ fetal liver macrophages, respectively, so that *c-Maf*$^{+/+}$ erythroblasts were cocultured on *c-Maf*$^{-/-}$ central macrophages and vice versa. Surprisingly, *c-Maf*$^{-/-}$ macrophages failed to support erythroblastic islands with the inoculated wild-type

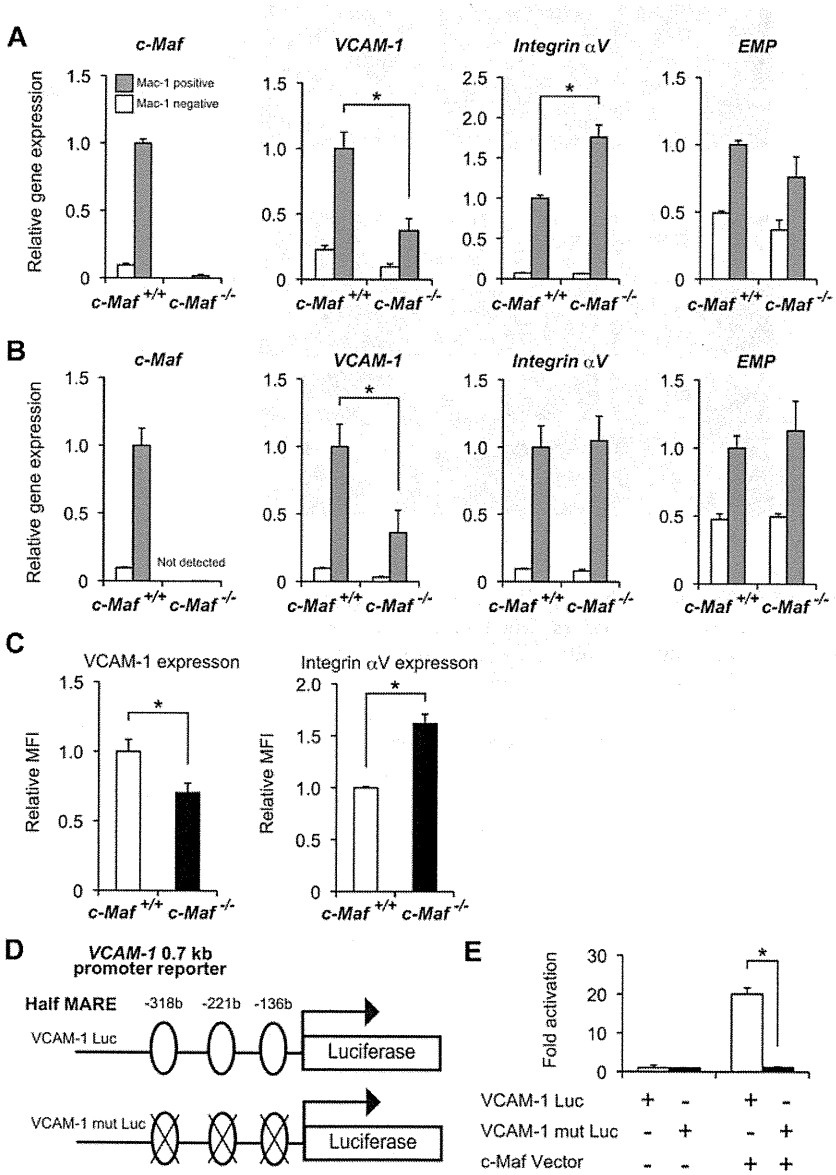

Figure 5. Decreased expression of VCAM-1 in *c-Maf*$^{-/-}$ fetal liver macrophage. mRNA expression profiles of erythroblast-macrophage adhesive interaction genes at E13.5 (A) and at E14.5 (B). Total RNA obtained from the Mac-1^{+} fraction (gray bar) and Mac-1^{-} fraction (open bar) of fetal liver cells was used for analyses. VCAM-1 expression was decreased in *c-Maf*$^{-/-}$ macrophages at E13.5 and E14.5; n = 7 per group; $^{*}P < .05$. The expression level of *c-Maf*$^{+/+}$ fetal liver Mac-1 fraction was set to 1.0. All of the data are presented as mean ± SEM (C) Relative mean fluorescent intensity (MFI) values of VCAM-1 and Integrin αV for the *c-Maf*$^{+/+}$ fetal liver Mac-1 fraction (normalized to MFI = 1) and the *c-Maf*$^{-/-}$ fetal liver Mac-1 fraction. E13.5 fetal liver cells were stained with FITC-conjugated anti–Mac-1 mAb, APC-conjugated anti–VCAM-1 mAb, and PE-conjugated anti-Integrin αV mAb. Bar graphs represent mean ratio ± SEM. Consistent with real-time RT-PCR analysis, significant differences in VCAM-1 and Integrin αV protein expression were observed; n = 8 per group; $^{*}P < .05$. (D) Schematic diagram of a luciferase reporter construct with the use of a VCAM-1 0.7-kb promoter (VCAM-1 Luc, top) ligated to a firefly luciferase cassette. Three putative half-MARE sites (5′ −318 bp, −221 bp, and −136 bp) are indicated. A luciferase assay was performed with a VCAM-1 Luc and that with mutations in half-MARE (VCAM-1 mut Luc, bottom) as reporters. (E) The pEFX3-FLAG-cMaf expression vector (c-Maf Vector) was cotransfected with the reporter plasmid into the macrophage cell line J774. The relative luciferase activity shown is derived from averages of 2 independent experiments (shown as mean ± SEM). The luciferase activity seen in J774 cells transfected with the reporter plasmid and with an empty vector was normalized to a value of 1 as the standard ($^{*}P < .05$).

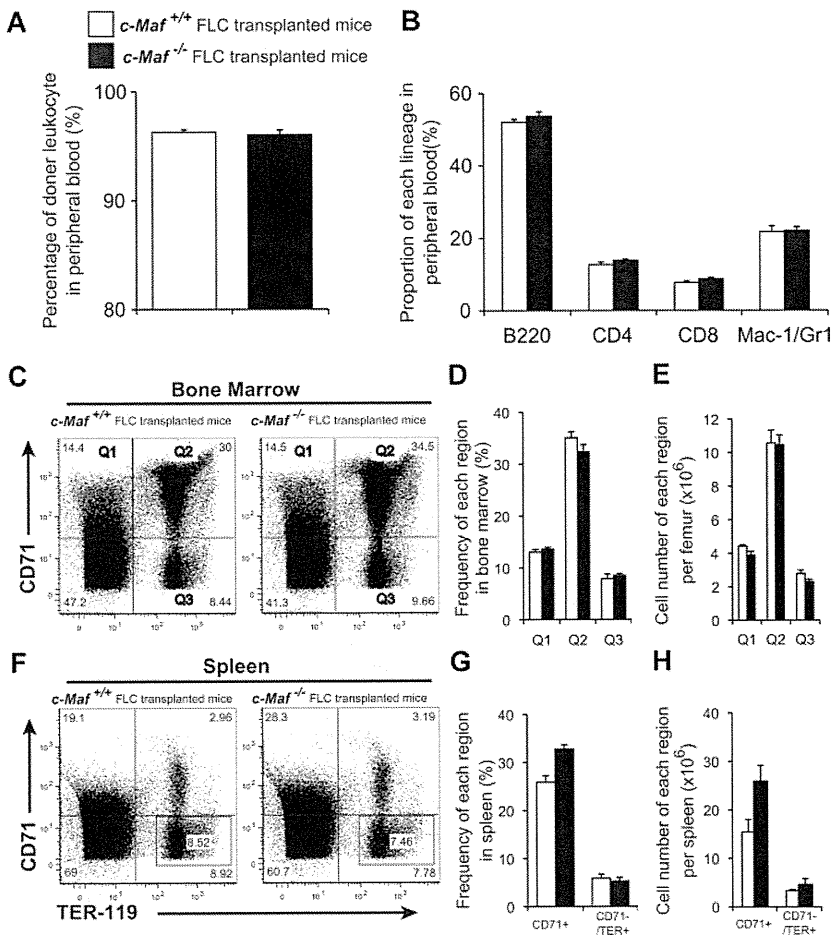

Figure 6. *c-Maf*$^{-/-}$ fetal liver cells can reconstitute adult hematopoiesis in lethally irradiated mice. (A) Eight to 10 weeks after transplantation, the donor leukocyte chimerism of the mice reconstituted with *c-Maf*$^{-/-}$ fetal liver cells was comparable to that of the mice reconstituted with *c-Maf*$^{+/+}$ fetal liver cells. The reconstitution efficiency was checked by flow cytometry with the use of the Ly5.1/Ly5.2 ratio of peripheral blood cells. Donor chimerism was determined to be as follows: (%Ly5.1$^+$/%Ly5.1$^+$ + %Ly5.2$^+$) × 100. (B) No significant difference was found in the proportion of each lineage in peripheral blood between *c-Maf*$^{+/+}$ fetal liver cells transplanted into mice and *c-Maf*$^{-/-}$ fetal liver cells transplanted into mice. (C) Flow cytometric analyses of the TER-119 and CD71 expression in total BM cells prepared from the femur of mice that received a transplant with *c-Maf*$^{+/+}$ fetal liver cells (left) or *c-Maf*$^{-/-}$ fetal liver cells (right). The gates of CD71$^+$/TER-119$^-$ (top left region: Q1), CD71$^+$/TER-119$^+$ (top right region: Q2), and CD71$^-$/TER-119$^+$ (bottom right region: Q3) in BM cells are defined as indicated. (D) Frequencies (%) of cells found in each region are shown. (E) Cell numbers of each region per femur are shown. (F) Flow cytometric analyses of the TER-119 and CD71 expression in total spleen cells prepared from mice that received a transplant with *c-Maf*$^{+/+}$ fetal liver cells (left) and *c-Maf*$^{-/-}$ fetal liver cells (right). The frequencies (%) of CD71$^+$ (top left and top right regions) and CD71$^-$/TER-119$^+$ (indicated squared gate in the bottom right region) cells in the spleen are indicated. (G) Frequencies (%) of each region are shown. (H) Cell numbers of each region per spleen are shown. Note that there are no significantly different frequencies or numbers of BM or spleen cells between mice that received a transplant with *c-Maf*$^{+/+}$ fetal liver cells versus with *c-Maf*$^{-/-}$ fetal liver cells. □ represents mice that received a transplant with *c-Maf*$^{+/+}$ fetal liver cells; ■, mice that received a transplant with *c-Maf*$^{-/-}$ fetal liver cells; n = 4 per group. FLC indicates, fetal liver cell.

erythroblasts (12.7 ± 0.5 erythroblasts per *c-Maf*$^{+/+}$ macrophage and 4.8 ± 0.2 erythroblasts per *c-Maf*$^{-/-}$ macrophage; Figure 4B). In contrast, *c-Maf*$^{-/-}$ erythroblasts were still capable of attaching to *c-Maf*$^{+/+}$ macrophages to the same extent as wild-type erythroblasts (13.9 ± 0.5 erythroblasts per *c-Maf*$^{+/+}$ macrophage and 5.1 ± 0.4 erythroblasts per *c-Maf*$^{-/-}$ macrophage; Figure 4C). These results show that the erythropoietic defects in *c-Maf*$^{-/-}$ embryos could be induced by an impaired hematopoietic microenvironment. Most probably, the suppressed functions of c-Maf–deficient central macrophages were responsible for the damaged erythroblastic islands.

Identification of target genes of c-Maf in fetal liver macrophages

To identify the molecular targets by which c-Maf regulates formation of erythroblastic islands in macrophages, we monitored the expression of cell adhesion molecules by microarray analysis. The expression of several important adhesion molecules was decreased in *c-Maf*$^{-/-}$ macrophages (Table 2). Expression of *VCAM-1* was suppressed the furthest in these molecules. To confirm the results from microarray analysis, we performed quantitative RT-PCR analyses, examining expression levels of *VCAM-1*, *Integrin* α*V*, and *EMP*. These are essential for erythroblastic island formation and maintenance and are thus designated as erythroblast-macrophage adhesive molecules.[3] The Mac-1$^+$ cells from either E13.5 or E14.5 fetal liver were sorted and analyzed to determine the mRNA abundance of these genes by real-time RT-PCR analysis. Of note, we observed an ~ 2.5-fold reduction in the *VCAM-1* mRNA expression level in the Mac-1$^+$ fraction from *c-Maf*$^{-/-}$ fetal liver, compared with the *c-Maf*$^{+/+}$ control at E13.5 and E14.5 (Figure 5A-B). However, *EMP* mRNA expression was not reduced in *c-Maf*$^{-/-}$ compared with *c-Maf*$^{+/+}$ (Figure 5A-B). In addition, expression of *Integrin* α*V* at E13.5 in *c-Maf*$^{-/-}$ was significantly up-regulated. Consistent with this observation, flow cytometric analysis of the fetal liver cells at E13.5 also verified a significant reduction of VCAM-1 protein expression in the *c-Maf*$^{-/-}$ fetal liver Mac-1$^+$ cells compared with the *c-Maf*$^{+/+}$ fetal liver Mac-1$^+$ cells, and protein expression of Integrin αV in the *c-Maf*$^{-/-}$ fetal liver Mac-1$^+$ cells was higher than that in *c-Maf*$^{+/+}$ (Figure 5C).

Given the significant suppression of VCAM-1 expression in *c-Maf*$^{-/-}$ fetal liver macrophages, we next addressed whether c-Maf could activate the *VCAM-1* gene promoter. To this end, a luciferase reporter assay in the J774 macrophage cell line was performed with a plasmid containing the 0.7-kb *VCAM-1* promoter region (VCAM-1 Luc) as a reporter (Figure 5D). The luciferase activity was significantly increased when the reporter plasmid was cotransfected with an expression plasmid for c-Maf. In contrast, when putative half-MARE sequences were mutated (VCAM-1 mut Luc), activation of the reporter was blunted (Figure 5E). These results indicate that c-Maf regulates the expression of *VCAM-1* by binding the putative half-MARE sites in its promoter region.

Table 3. Blood cell counts 6-12 weeks after fetal liver cell transplantation in mice

Genotype of transplanted FLC	*c-Maf*$^{+/+}$	*c-Maf*$^{-/-}$
WBC count, /μL	14 100 ± 1500	13 500 ± 1400
RBC count, ×10^4/μL	967 ± 10.0	949 ± 11.0
Hb level, g/dL	14.1 ± 0.2	13.9 ± 0.2
HCT, %	47.1 ± 0.7	46.8 ± 0.7
MCV, fL	48.7 ± 0.5	49.3 ± 0.4
MCH, pg	14.6 ± 0.2	14.6 ± 0.1
PLT count, ×10^4/μL	102.6 ± 5.8	92.3 ± 4.6

Values shown are the mean ± SEM for 20 mice per genotype. Mice with ≥ 90% donor leukocyte chimerism were used for analysis. *P* values were all NS.

FLC indicates fetal liver cell; WBC, white blood cell; RBC, red blood cell; Hb, hemoglobin; HCT, hematocrit; MCV, mean corpuscular volume; MCH, mean corpuscular hemoglobin; and PLT, platelet.

c-Maf–deficient fetal liver cells are capable of reconstituting the hematopoietic system of adult mice

To determine whether *c-Maf*$^{-/-}$ embryos still retain functional hematopoietic stem cells, we tested the ability of *c-Maf*–deficient fetal liver cells to reconstitute the hematopoietic system of lethally irradiated recipient mice. Fetal liver cells collected from E14.5 *c-Maf*$^{+/+}$ or *c-Maf*$^{-/-}$ embryos were injected into lethally irradiated recipient mice. All recipients receiving both *c-Maf*$^{+/+}$ and *c-Maf*$^{-/-}$ fetal liver cells survived and remained healthy for ≥ 6 months after transplantation. The donor-derived leukocyte chimerism in the mice reconstituted with *c-Maf*$^{-/-}$ fetal liver cells was comparable with that of the recipient mice with control fetal liver cells (Figure 6A). Moreover, there were no significant differences in hematocrit or proportion (%) of B220$^+$, CD4$^+$, CD8$^+$, or Mac-1$^+$/Gr1$^+$ cells between the recipients receiving *c-Maf*$^{+/+}$ or *c-Maf*$^{-/-}$ fetal liver cells (Table 3; Figure 6B).

Next, we attempted to examine whether erythroblast differentiation in the BM and spleen was perturbed. The absolute number of BM cells (19.9 ± 1.69 and 18.3 ± 1.56 × 10^6 cells/femur for *c-Maf*$^{+/+}$ and *c-Maf*$^{-/-}$ fetal liver cells transplanted into mice, respectively) as well as the spleen weight (68.4 ± 3.28 and 73.8 ± 5.44 mg for *c-Maf*$^{+/+}$ and *c-Maf*$^{-/-}$ fetal liver cells transplanted into mice, respectively) were comparable between mice that received a transplant with *c-Maf*$^{+/+}$ and *c-Maf*$^{-/-}$ fetal liver cells. Each stage of the erythroblasts was prospectively separated by a flow cytometric protocol that used TER-119 and CD71 Abs. The frequencies and cell numbers of each region in the recipient BM receiving *c-Maf*$^{-/-}$ fetal liver cells were comparable to those in the recipient with *c-Maf*$^{+/+}$ fetal liver cells (Figure 6C-E). Similar results were also observed with spleen cells (Figure 6F-H). Applying another method that TER-119 and CD44 Abs,[30] we assessed erythropoiesis in the BM of the mice that received a transplant. The differentiation status was found to be comparable between the recipients with *c-Maf*$^{+/+}$ and *c-Maf*$^{-/-}$ fetal liver cells (supplemental Figure 5A-C). Overall, these results indicate that *c-Maf*$^{-/-}$ hematopoietic cells are able to reconstitute the hematopoietic system in lethally irradiated mice and that they have the ability to produce adequate amounts of erythroid cells.

c-Maf deficiency does not impair erythropoiesis during PHZ-induced anemia

To assess the role of c-Maf in adult hematopoiesis further, we analyzed BM macrophages in a similar manner as that used to analyze fetal liver cells. The donor-derived BM leukocyte and BM macrophage chimerisms in the mice reconstituted with *c-Maf*$^{-/-}$ fetal liver cells were comparable with those of the recipient mice with control fetal liver cells (supplemental Figure 6). To determine whether *VCAM-1* mRNA levels were decreased, Mac-1$^+$ cells from the BM of mice that received a transplant were sorted and analyzed for mRNA abundance of *Mac-1*, *c-Maf*, *VCAM-1*, and *Integrin* α*V* by real-time RT-PCR analysis. These experiments showed no differences in expression levels in mice that received a transplant with *c-Maf*$^{+/+}$ and *c-Maf*$^{-/-}$ fetal liver cells except for *c-Maf* (Figure 7A), in contrast to the results obtained with the use of fetal

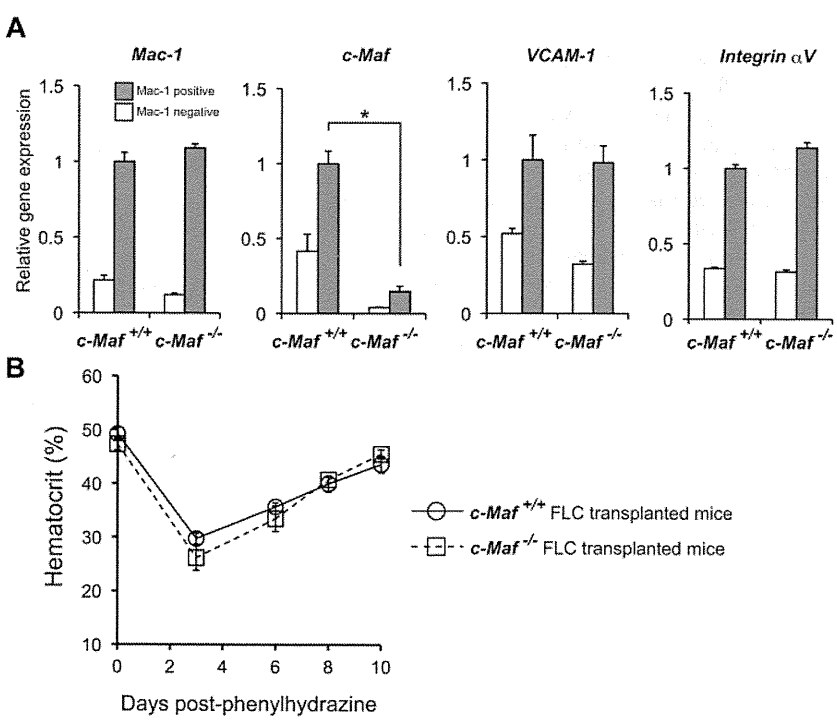

Figure 7. Responses of mice that received a transplant with *c-Maf*$^{-/-}$ fetal liver cells to induce anemia. (A) Comparisons of mRNA expression of *Mac-1*, *c-Maf*, *VCAM-1*, and *Integrin* α*V* are shown. Total RNA obtained from the Mac-1$^+$ positive fraction (gray bar) and the Mac-1$^-$ fraction (open bar) of BM cells was used for analyses. Note that *VCAM-1* mRNA expression of the Mac-1$^+$ fraction in mice that received a transplant with *c-Maf*$^{-/-}$ fetal liver cells is comparable with that of control mice that received a transplant with *c-Maf*$^{+/+}$ fetal liver cells; n = 5 per group; FLC indicates fetal liver cell; Expression of the *c-Maf*$^{+/+}$ BM Mac-1 fraction was set to 1.0. All of the data are presented as mean ± SEM. (B) Mice with a baseline hematocrit of ≥ 35% were used. Four mice that received a transplant with *c-Maf*$^{+/+}$ fetal liver cells (open circle with solid line) and 4 mice that received a transplant with *c-Maf*$^{-/-}$ fetal liver cells (open square with dashed line) were injected with phenylhydrazine on days 0, 1, and 3. Hematocrit levels were assessed on days 0, 3, 6, 8, and 10. Data are mean ± SEM.

liver cells. To reconfirm these results with a functional assay, mice were challenged with PHZ, and their hematocrits were monitored for the next 10 days (Figure 7B). The hematocrits of mice from both groups were comparable during this period. These results indicate that c-Maf deficiency does not impair stress erythropoiesis during PHZ-induced anemia in adult mice.

Discussion

Macrophages are important for hematopoiesis because they engulf nuclei of erythroblasts in erythroblastic islands, where the macrophages are surrounded by erythroblasts in the fetal liver, BM, and spleen.[3] In the present study, we demonstrated that c-Maf is crucial for the function of macrophages in erythropoiesis.

Our study clearly shows that disruption of c-Maf causes impaired erythroblastic island formation because of dysfunction of fetal liver macrophages. In a methylcellulose culture system, *c-Maf*$^{-/-}$ hematopoietic stem/progenitor cells in fetal liver have a normal potential to differentiate into different lineages, and they can reconstitute the hematopoietic system of lethally irradiated mice. Because c-Maf is specifically expressed in macrophages within the fetal liver, it has been thought that c-Maf does not regulate fetal liver erythropoiesis through a function of erythroblasts, but rather that it performs an adhesive function of macrophages. There are several reports of genes that are related to the formation and maintenance of erythroblastic islands, based on the knockout mice technique. Retinoblastoma-deficient mice were analyzed for macrophage differentiation, and erythroblastic island formation was reported to be impaired in these mice.[31] The fetal livers of *Dnase2a*$^{-/-}$ mice contain many macrophages that carry undigested DNA, and IFN-β mRNA was expressed by the resident macrophages in the *Dnase2a*$^{-/-}$ fetal liver.[37,38] In *c-Maf*$^{-/-}$ fetal livers, retinoblastoma was comparably expressed in *c-Maf*$^{+/+}$ and *c-Maf*$^{-/-}$ macrophages; therefore, the existence of impaired erythroblastic islands in *c-Maf*$^{-/-}$ mice is not related to retinoblastoma (supplemental Figure 7). In addition, we could not detect the abnormal foci that are found in *Dnase2a*$^{-/-}$ fetal livers or the expression of *IFN*-β mRNA (data not shown). Thus, retinoblastoma or DNase II do not cause the impaired erythroblastic islands of *c-Maf*$^{-/-}$ embryos.

To identify the target genes of c-Maf in fetal liver macrophages, we performed microarray analysis and found that VCAM-1 was one of these target genes. VCAM-1 is an adhesion molecule expressed on macrophages of erythroblastic islands. Previous studies have shown that maintenance of erythroblastic islands was impaired by an anti–VCAM-1 Ab.[8,39] As shown in Figure 5, mRNA and cell surface protein expression of VCAM-1 was decreased in *c-Maf*$^{-/-}$ fetal liver macrophages. This suggests that decreased expression of *VCAM-1* may be at least in part responsible for impaired erythroblastic island maintenance in *c-Maf*$^{-/-}$ fetal liver. The large Maf proteins are known to bind MAREs or the 5′ AT-rich half-MARE. In the *VCAM-1* promoter region, there are 3 half-MARE sites, so c-Maf may directly regulate *VCAM-1* expression in fetal liver macrophages. Recently, Kohyama et al[40] revealed that Spi-C controls the development of red pulp macrophages required for red blood cell recycling, and it regulates *VCAM-1* expression in red pulp macrophages. These earlier results and ours suggest that the regulation of *VCAM-1* expression by transcription factors strongly affects the function of tissue macrophages. In macrophages, c-Maf regulates the expression of cell surface molecules that are involved in macrophage function. In this analysis, expression of Integrin αV in *c-Maf*$^{-/-}$ macrophages was transiently up-regulated. It is difficult to identify the mechanism, but it seems probable there may be a compensation mechanism causing down-regulation of VCAM-1 in fetal macrophages.

We found that c-Maf is crucial for erythroblastic island maintenance in the embryonic stage. In a reconstitution assay that used fetal liver cells, *c-Maf*$^{-/-}$ hematopoietic cells reconstituted hematopoiesis in lethally irradiated mice, and the mice that received a transplant with *c-Maf*$^{-/-}$ fetal liver cells did not show anemia in the steady state (Table 3). To test the function of c-Maf in the adult stage further, we analyzed the mice that received a transplant by BM cell assay and by a PHZ stress test. Neither decreased expression level of *VCAM-1* mRNA nor impaired erythroid differentiation were observed. In addition, the response to the PHZ stress test was also comparable between the 2 groups. These results indicate that c-Maf might activate the VCAM-1 gene and affect erythroblastic island maintenance in a context-dependent manner. Such observations were reported previously. In *Palld*$^{-/-}$ fetal liver, erythroblastic island formation or integrity was impaired, but *Palld*$^{-/-}$ fetal liver cells could reconstitute the blood of lethally irradiated mice.[6] Thus, c-Maf and Palladin are important for erythroblastic islands in the embryonic stage, but their importance in the adult stage is still unconfirmed. However, a previous study found that ICAM-4 is critical for erythroblastic island formation in adult marrow,[41] but the role of ICAM-4 in the embryonic stage has been left for future study. Overall, previous studies and our results indicate that there might be different mechanisms or regulation processes or both between fetal liver and adult marrow/spleen erythroblastic island formation and maintenance. This suggests that macrophages in fetal liver and in the adult marrow/spleen might have different developmental origins. Further studies are needed to investigate this possibility.

Recent reports have indicated that definitive as well as primitive erythropoiesis are related to erythroblastic islands.[39] Kingsley et al[42] revealed that yolk sac-derived primitive erythroblasts enucleate during gestation, and Isern et al[39] and Fraser et al[43] also have demonstrated, using transgenic mouse lines, that primitive erythroblasts enucleate within the fetal liver.[39,43] Our quantitative RT-PCR results suggested that definitive erythropoiesis is more involved in erythroblastic islands than is primitive erythropoiesis in vivo (supplemental Figure 3). Therefore, this result indicates that definitive erythropoiesis in fetal liver is predominantly impaired in *c-Maf*$^{-/-}$ embryos, whereas primitive erythropoiesis is maintained in *c-Maf*$^{-/-}$ embryos.

Our study showed that *c-Maf*$^{-/-}$ mice were embryonic lethal on the C57BL/6 background and that *c-Maf*$^{-/-}$ macrophages might be responsible for this. Previous reports from our laboratory and from others indicated that *c-Maf*$^{-/-}$ mice were lethal around birth on the C57BL/6J × 129/SV background, but some mice on the BALB/c background live to adulthood.[14,44,45] It is known that cytokine production in T-helper cells differs between C57BL/6 and BALB/c backgrounds. Recently Mills at al[46] reported that cytokine production in macrophages differed according to the backgrounds of the mice. On a C57BL/6 background, inflammatory cytokine production is more dominant than on a BALB/c background. It is well known that apoptotic cells are recognized by macrophages and induce the production of proinflammatory cytokines.[47] Increased amounts of apoptotic cells were observed in *c-Maf*$^{-/-}$ fetal liver, suggesting that inflammatory cytokine production might be triggered in *c-Maf*$^{-/-}$ fetal liver. Therefore, our *c-Maf*$^{-/-}$ mice were lethal at an earlier gestational date than indicated by previous reports. We found that *c-Maf*$^{-/-}$ fetal liver macrophages produced

more cytokines than *c-Maf*$^{+/+}$ fetal liver macrophages (supplemental Figure 7). Hence, it is tempting to speculate that increased numbers of apoptotic cells trigger the production of inflammatory cytokines that are reported to be responsible for anemia and embryonic lethality. This speculation supports the idea that the *c-Maf*$^{-/-}$ macrophages are responsible for anemia and lethality. This hypothesis may also explain the phenotype discrepancy between *c-Maf*$^{-/-}$ mice and *F4/80*$^{-/-}$ or *VCAM-1*$^{-/-}$ mice. Neither F4/80 knockout mice nor mice with a conditional ablation of VCAM-1 in blood cells are embryonic lethal.[48-50] In addition, c-Maf is a transcription factor, and it might regulate sets of target genes in fetal macrophages that might in turn be responsible for the observed anemia and lethality.

In summary, we have shown that the transcription factor c-Maf gene affects the hematopoietic microenvironment by playing a crucial role in regulating fetal liver macrophages.

Acknowledgments

The authors thank Dr Yamashita and Dr Ohneda for the *VCAM-1* promoter containing luciferase plasmid.

This work was supported by a Grant-in-Aid for Scientific Research (KAKENHI no. 21220009) from the Ministry of Education, Culture, Sports, Science and Technology of Japan (MEXT). This work was also supported by Grants from the Astellas Foundation for Research on Metabolic Disorders and the Uehara Memorial Foundation. M.K. is a recipient of a Japan Society for the Promotion of Science Research Fellowship for Young Scientists (21384).

Authorship

Contribution: M.K., K.H., M.H., M.N., T.O., H.S., and M.T.N.T. performed experiments; M.K., K.H., and M.H. analyzed results and made figures; M.K., K.H., M.H., and S.T. designed the research; M.K., M.H., and S.T. wrote the paper; K.U. performed microarray analysis; and T.K., H.N., S.C., and S.T. supervised the project.

Conflict-of-interest disclosure: The authors declare no competing financial interests.

Correspondence: Satoru Takahashi, Departments of Anatomy and Embryology, Institute of Basic Medical Science, University of Tsukuba, 1-1-1 Tennodai, Tsukuba, Ibaraki 305-8575, Japan; e-mail: satoruta@md.tsukuba.ac.jp.

References

1. Palis J. Ontogeny of erythropoiesis. *Curr Opin Hematol.* 2008;15(3):155-161.
2. Allen TD, Dexter TM. Ultrastructural aspects of erythropoietic differentiation in long-term bone marrow culture. *Differentiation.* 1982;21(2):86-94.
3. Chasis JA, Mohandas N. Erythroblastic islands: niches for erythropoiesis. *Blood.* 2008;112(3):470-478.
4. Hanspal M, Hanspal JS. The association of erythroblasts with macrophages promotes erythroid proliferation and maturation: a 30-kD heparin-binding protein is involved in this contact. *Blood.* 1994;84(10):3494-3504.
5. Mohandas N, Prenant M. Three-dimensional model of bone marrow. *Blood.* 1978;51(4):633-643.
6. Liu X-S, Li X-H, Wang Y, et al. Disruption of palladin leads to defects in definitive erythropoiesis by interfering with erythroblastic island formation in mouse fetal liver. *Blood.* 2007;110(3):870-876.
7. Soni S, Bala S, Gwynn B, Sahr KE, Peters LL, Hanspal M. Absence of erythroblast macrophage protein (Emp) leads to failure of erythroblast nuclear extrusion. *J Biol Chem.* 2006;281(29):20181-20189.
8. Sadahira Y, Yoshino T, Monobe Y. Very late activation antigen 4-vascular cell adhesion molecule 1 interaction is involved in the formation of erythroblastic islands. *J Exp Med.* 1995;181(1):411-415.
9. Nishizawa M, Kataoka K, Goto N, Fujiwara KT, Kawai S. v-maf, a viral oncogene that encodes a "leucine zipper" motif. *Proc Natl Acad Sci U S A.* 1989;86(20):7711-7715.
10. Kataoka K, Fujiwara KT, Noda M, Nishizawa M. MafB, a new Maf family transcription activator that can associate with Maf and Fos but not with Jun. *Mol Cell Biol.* 1994;14(11):7581-7591.
11. Kataoka K, Noda M, Nishizawa M. Maf nuclear oncoprotein recognizes sequences related to an AP-1 site and forms heterodimers with both Fos and Jun. *Mol Cell Biol.* 1994;14(1):700-712.
12. Yoshida T, Ohkumo T, Ishibashi S, Yasuda K. The 5′-AT-rich half-site of Maf recognition element: a functional target for bZIP transcription factor Maf. *Nucleic Acids Res.* 2005;33(11):3465-3478.
13. Kajihara M, Kawauchi S, Kobayashi M, Ogino H, Takahashi S, Yasuda K. Isolation, characterization, and expression analysis of zebrafish large Mafs. *J Biochem.* 2001;129(1):139-146.
14. Kawauchi S, Takahashi S, Nakajima O, et al. Regulation of lens fiber cell differentiation by transcription factor c-Maf. *J Biol Chem.* 1999;274(27):19254-19260.
15. Moriguchi T, Hamada M, Morito N, et al. MafB is essential for renal development and F4/80 expression in macrophages. *Mol Cell Biol.* 2006;26(15):5715-5727.
16. Ogino H, Yasuda K. Induction of lens differentiation by activation of a bZIP transcription factor, L-Maf. *Science.* 1998;280(5360):115-118.
17. Sieweke MH, Tekotte H, Frampton J, Graf T. MafB is an interaction partner and repressor of Ets-1 that inhibits erythroid differentiation. *Cell.* 1996;85(1):49-60.
18. Swaroop A, Xu JZ, Pawar H, Jackson A, Skolnick C, Agarwal N. A conserved retina-specific gene encodes a basic motif/leucine zipper domain. *Proc Natl Acad Sci U S A.* 1992;89(1):266-270.
19. Zhang C, Moriguchi T, Kajihara M, et al. MafA is a key regulator of glucose-stimulated insulin secretion. *Mol Cell Biol.* 2005;25(12):4969-4976.
20. Eychene A, Rocques N, Pouponnot C. A new MAFia in cancer. *Nat Rev Cancer.* 2008;8(9):683-693.
21. Hurt EM, Wiestner A, Rosenwald A, et al. Overexpression of c-maf is a frequent oncogenic event in multiple myeloma that promotes proliferation and pathological interactions with bone marrow stroma. *Cancer Cell.* 2004;5(2):191-199.
22. Morito N, Yoh K, Fujioka Y, et al. Overexpression of c-Maf contributes to T-cell lymphoma in both mice and human. *Cancer Res.* 2006;66(2):812-819.
23. Murakami YI, Yatabe Y, Sakaguchi T, et al. c-Maf expression in angioimmunoblastic T-cell lymphoma. *Am J Surg Pathol.* 2007;31(11):1695-1702.
24. Bauquet AT, Jin H, Paterson AM, et al. The costimulatory molecule ICOS regulates the expression of c-Maf and IL-21 in the development of follicular T helper cells and TH-17 cells. *Nat Immunol.* 2009;10(2):167-175.
25. Ho IC, Hodge MR, Rooney JW, Glimcher LH. The proto-oncogene c-maf is responsible for tissue-specific expression of interleukin-4. *Cell.* 1996;85(7):973-983.
26. Cao S, Liu J, Song L, Ma X. The protooncogene c-Maf is an essential transcription factor for IL-10 gene expression in macrophages. *J Immunol.* 2005;174(6):3484-3492.
27. Aziz A, Soucie E, Sarrazin S, Sieweke MH. MafB/c-Maf deficiency enables self-renewal of differentiated functional macrophages. *Science.* 2009;326(5954):867-871.
28. Nakamura M, Hamada M, Hasegawa K, et al. c-Maf is essential for the F4/80 expression in macrophages in vivo. *Gene.* 2009;445(1-2):66-72.
29. Masuoka HC, Townes TM. Targeted disruption of the activating transcription factor 4 gene results in severe fetal anemia in mice. *Blood.* 2002;99(3):736-745.
30. Chen K, Liu J, Heck S, Chasis JA, An X, Mohandas N. Resolving the distinct stages in erythroid differentiation based on dynamic changes in membrane protein expression during erythropoiesis. *Proc Natl Acad Sci U S A.* 2009;106(41):17413-17418.
31. Iavarone A, King ER, Dai X-M, Leone G, Stanley ER, Lasorella A. Retinoblastoma promotes definitive erythropoiesis by repressing Id2 in fetal liver macrophages. *Nature.* 2004;432(7020):1040-1045.
32. Ema M, Mori D, Niwa H, et al. Kruppel-like factor 5 is essential for blastocyst development and the normal self-renewal of mouse ESCs. *Cell Stem Cell.* 2008;3(5):555-567.
33. Yamashita T, Ohneda O, Sakiyama A, Iwata F, Ohneda K, Fujii-Kuriyama Y. The microenvironment for erythropoiesis is regulated by HIF-2alpha through VCAM-1 in endothelial cells. *Blood.* 2008;112(4):1482-1492.
34. Angelillo-Scherrer A, Burnier L, Lambrechts D, et al. Role of Gas6 in erythropoiesis and anemia in mice. *J Clin Invest.* 2008;118(2):583-596.
35. Wu L, de Bruin A, Saavedra HI, et al. Extra-embryonic function of Rb is essential for embryonic development and viability. *Nature.* 2003;421(6926):942-947.
36. Zhang J, Socolovsky M, Gross AW, Lodish HF.

Role of Ras signaling in erythroid differentiation of mouse fetal liver cells: functional analysis by a flow cytometry-based novel culture system. *Blood.* 2003;102(12):3938-3946.

37. Kawane K, Fukuyama H, Kondoh G, et al. Requirement of DNase II for definitive erythropoiesis in the mouse fetal liver. *Science.* 2001;292(5521): 1546-1549.
38. Yoshida H, Okabe Y, Kawane K, Fukuyama H, Nagata S. Lethal anemia caused by interferon-beta produced in mouse embryos carrying undigested DNA. *Nat Immunol.* 2005;6(1):49-56.
39. Isern J, Fraser ST, He Z, Baron MH. The fetal liver is a niche for maturation of primitive erythroid cells. *Proc Natl Acad Sci U S A.* 2008;105(18): 6662-6667.
40. Kohyama M, Ise W, Edelson BT, et al. Role for Spi-C in the development of red pulp macrophages and splenic iron homeostasis. *Nature.* 2009;457(7227):318-321.
41. Lee G, Lo A, Short SA, et al. Targeted gene deletion demonstrates that the cell adhesion molecule ICAM-4 is critical for erythroblastic island formation. *Blood.* 2006;108(6):2064-2071.
42. Kingsley PD, Malik J, Fantauzzo KA, Palis J. Yolk sac-derived primitive erythroblasts enucleate during mammalian embryogenesis. *Blood.* 2004; 104(1):19-25.
43. Fraser ST, Isern J, Baron MH. Maturation and enucleation of primitive erythroblasts during mouse embryogenesis is accompanied by changes in cell-surface antigen expression. *Blood.* 2007;109(1):343-352.
44. Kim JI, Li T, Ho IC, Grusby MJ, Glimcher LH. Requirement for the c-Maf transcription factor in crystallin gene regulation and lens development. *Proc Natl Acad Sci U S A.* 1999;96(7):3781-3785.
45. Ring BZ, Cordes SP, Overbeek PA, Barsh GS. Regulation of mouse lens fiber cell development and differentiation by the Maf gene. *Development.* 2000;127(2):307-317.
46. Mills CD, Kincaid K, Alt JM, Heilman MJ, Hill AM. M-1/M-2 macrophages and the Th1/Th2 paradigm. *J Immunol.* 2000;164(12):6166-6173.
47. Nagata S, Hanayama R, Kawane K. Autoimmunity and the clearance of dead cells. *Cell.* 2010; 140(5):619-630.
48. Lin HH, Faunce DE, Stacey M, et al. The macrophage F4/80 receptor is required for the induction of antigen-specific efferent regulatory T cells in peripheral tolerance. *J Exp Med.* 2005;201(10): 1615-1625.
49. Schaller E, Macfarlane AJ, Rupec RA, Gordon S, McKnight AJ, Pfeffer K. Inactivation of the F4/80 glycoprotein in the mouse germ line. *Mol Cell Biol.* 2002;22(22):8035-8043.
50. Ulyanova T, Scott LM, Priestley GV, et al. VCAM-1 expression in adult hematopoietic and nonhematopoietic cells is controlled by tissue-inductive signals and reflects their developmental origin. *Blood.* 2005;106(1):86-94.